Electronic Supplementary Material (ESI) for RSC Advances.


# Synthesis and Electronic Properties of Pyridine End-capped Cyclopentadithiophene-Vinylene Oligomers

Fernando G. Guijarro[a, †], Samara Medina Rivero[b, †], Suman Gunasekaran[c], Iratxe Arretxea[b], Rocío Ponce Ortiz[b], Rubén Caballero[a], Pilar de la Cruz[a], Fernando Langa*[,a], Latha Venkataraman*[,c,d], Juan Casado*[,b]

[a] Instituto de Nanociencia Molecular (INAMOL), Universidad de Castilla-la Mancha, Toledo, Spain

[b] Department of Physical Chemistry, University of Malaga Campus de Teatinos s/n, 229071 Malaga, Spain,

[c] Department of Chemistry, Columbia University, New York, New York 10027, United States

[d] Department of Applied Physics and Applied Mathematics, Columbia University, New York, New York 10027, United States

[†] These authors contributed equally to this work.

## Table of Contents

## Part 1. General Information

**Materials.** Solvents and chemicals were purchased from Aldrich Chemicals (Milwaukee, WI). Anhydrous solvents, where indicated, were dried using a Pure-Sov 400 or using standard techniques.

**General Methods.** Chromatographic purifications were performed using silica gel 60 VWR (particle size 0.040-0.063 mm). Analytical thin-layer chromatography was performed using Merck TLC silica gel 60 F254. $^{1}$H NMR spectra were recorded as solutions in a partial deuterated solvent on a Brüker-Topspin AV 400 instrument. Chemical shifts are given as δ values. $^{1}$H NMR chemical shifts are reported relative to residual non deuterated solvent peaks. $^{13}$C NMR chemical shifts are reported relative to the deuterated solvent peak. FT-IR spectra were recorded in an AVATAR 370 FT-IR Thermo Nicolet spectrometer. Mass spectra (MALDI-TOF) were recorded on a VOYAGER DETM STR mass spectrometer using dithranol as matrix. Analytical HPLC profiles were recorded using Agilent 1260 (column: Buckyprep (4.6ID x 250 mm)). UV/Vis spectra were recorded on a Shimadzu UV-VIS-NIR spectrophotometer UV-3600 in quartz cuvettes with a path length of 1 cm. Fluorescene measurements were carried out on Cary Eclipse fluorescence spectrophotometer. Cyclic and Oyster-Young Square wave voltammetry were performed in a μAUTOLAB Type III potentiostat, using 0.1M solution of Tetrabutylammonium perchlorate in 1,2-dichlorobenzene:acetonitrile 4:1 as a supporting electrolite. Solutions were deoxygenated by bubbling argon through prior to each measurement which was run under an argon atmosphere. Experiments were carried out in a one-compartment cell equipped with a glassy carbon electrode, a platinum wire counter electrode and an $Ag/AgNO_3$ as pseudo reference electrode. All Potentials were checked against the ferrocene/ferrocenium couple (Fc/Fc+) after each experiment. Melting points are recorded in Gallenkamp melting point apparatus and are uncorrected. Thermogravimetric analyses were performed using a TGA/DSC Linea Excellent instrument by Mettler-Toledo and collected under inert atmosphere of nitrogen with a scan rate of 10 °C $min^{-1}$. The weight changes were recorded as a function of temperature.

**DFT Calculations.** DFT calculations performed with the GAUSSIAN 16 suite of programs[1]. Molecular geometry optimizations were performed with the B3LYP functional and the 6-31G** standard basis set[2-3]. Energy optimizations were performed by allowing all geometric parameters to vary independently. The optimum energy structures were found to be a true minimum in the ground state potential energy surface.

**Spectrochemical Experiment.** Titration and oxidation experiments have been conducted in dichloromethane at room temperature by progressive addition of trifluoroacetic acid (TFA; Sigma-Aldrich, reagent plus, 99%, CAS: 76-05-1) or $FeCl_3$, respectively, to a $10^{-6}$ M solution of the corresponding **PynCPDTV** oligomer. In situ UV-

Vis-NIR spectrochemical studies were conducted on the Varian Cary 5000 UV-Vis-NIR Spectrophotometer.

**Vapochromism Experiments**. UV-Vis electronic absorption spectra and 1064 nm FT-Raman spectra were performed in thin films formed by drop-coating deposition over a $SiO_2$ surface from $10^{-3}$ mol/L solution of the corresponding **PynCPDTV** oligomer in $CH_2Cl_2$. Pristine films were exposed to TFA vapors and electronic absorption and FT-Raman spectra were obtained. Finally, the protonated thin films were exposed to $NH_3$ vapors and measured again.

**Organic Field Effect Transistors.** Solution-processed OTFTs were fabricated by spin-coating of a 7 mg/mL solution in chloroform. Due to the hydrophobicity of the substrates, spreading of the solutions with the tip of the pipette helped to achieve a homogenous deposition. Prior to deposition, the wafers were cleaned by rinsing twice with EtOH followed by a 5 min plasma cleaning in a Harrick PDC-32G Plasma Cleaner/Sterilizer. Then, a self-assembled monolayer (SAM) of either hexamethyldisilazane (HMDS) was deposited in order to reduce charge trapping and thus enhance mobility. Treatment with hexamethyldisilazane was carried out by exposing the cleaned silicon wafers to HMDS vapor at room temperature in a closed air-free container under argon, whereas treatment with octadecyltrichlorosilane was performed by immersing the silicon wafers in a 3.0 mM humidity-exposed OTS-hexane solution for 1 hour, as previously described.

Top contact OFETs were fabricated by vapor deposition of gold electrodes (~$10^{-7}$ Torr, 0.2 Å/s, ~50 nm thick) onto the semiconductor thin films through a shadow mask to obtain devices with deliberately varied channel widths and lengths. The capacitance of the 300 nm $SiO_2$ gate insulator is 2 x $10^{-8}$ $Fcm^{-2}$. Characterization of the devices was performed under vacuum in a customized high-vacuum probe station (~$10^{-6}$ Torr) and in ambient atmosphere using an EB-4 Everbeing probe station with a 4200-SCS/C Keithley semiconductor characterization system.

## Part 2. Synthesis

**General procedure for Wittig reaction.** [4]

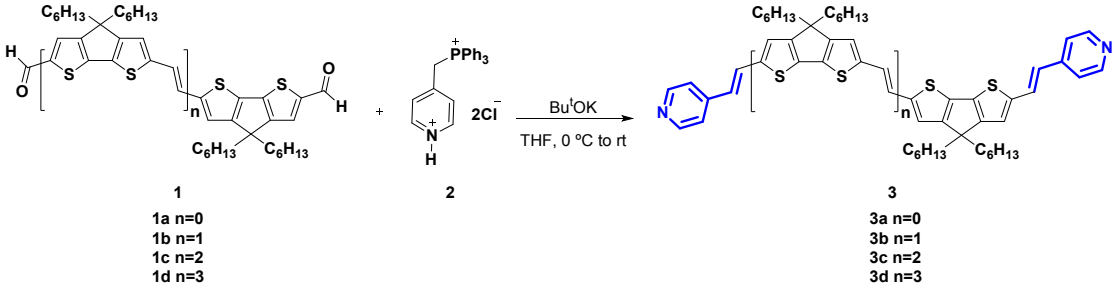


**Scheme S1.** General synthesis of **PynCPDTV** oligomers.

Under argon atmosphere, over a stirred solution of 4-methylphosphonium pyridinium dichloride **2**[5] in dry THF, at 0 °C, was added potassium *tert*-butoxide and the resulting solution was stirred for 30 min. Still at the same temperature the corresponding bisaldehyde was added portionwise and the resulting solution was allowed to warm to room temperature and stirred for the indicated time. After, the organic solvent was evaporated and the crude was redissolved in dichloromethane. The organic phase was washed with aqueous saturated $NaHCO_3$ and water, dried over anhydrous $Na_2SO_4$ and evaporated to dryness. Then crude was purified by chromatographic techniques to obtain **3a-d**.

**Synthesis of Py1CPDTV (3a).** According to the general procedure for Wittig reaction, using bisaldehyde **1a**[6] (100 mg, 0.24 mmol, 1 eq), 4-methylphosphonium pyridinium dichloride **2** (614 mg, 1.44 mmol, 6 eq), potassium *tert*-butoxide (485 mg, 4.32 mmol, 18 eq) and dry THF (30 mL). Reaction time: 17 hours. Purification: Column chromatography (Silica gel, Hexane:$CH_2Cl_2$:$Et_3N$ 48:48:3 and then $CH_2Cl_2$/MeOH 98:2) and gel permeation chromatography (Biobeads X1, Toluene) to obtain **3a** as a dark yellow solid with (100 mg, 75%). M.P.: 100-101 °C. FT-IR (KBr) ν/cm$^{-1}$: 3063, 3024, 2924, 2854, 1689, 1589, 1489, 1404, 1273, 1188, 1126, 949, 833, 802. $^1$H-NMR (400 MHz, $CD_2Cl_2$) δ/ppm: 8.52 (d, 4H, $^3J$=6.0 Hz), 7.47 (d, 2H, $^3J$=16.0 Hz), 7.33 (d, 4H, $^3J$=6.0 Hz), 7.06 (s, 2H), 6.82 (d, 2H, $^3J$=16.0 Hz), 1.87 (m, 4H), 1.19 (m, 16H), 0.81 (t, 6H, $^3J$=6.8 Hz). $^{13}$C-NMR (100 MHz, $CD_2Cl_2$) δ/ppm: 160.1, 150.5, 145.0, 143.7, 138.0, 127.4, 123.8, 123.3, 120.9, 54.6, 38.2, 32.2, 30.2, 25.1, 23.2, 14.4. MS (MALDI-TOF) *m/z*: calculated for $C_{35}H_{40}N_2S_2$: 552.263; found: 552.478[M+]. UV-Vis ($CH_2Cl_2$) $\lambda_{max}$/nm (log ε): 450 (4.45).

**Synthesis of Py2CPDTV (3b).** According to the general procedure for Wittig reaction, using bisaldehyde **1b**[6] (150 mg, 0.194 mmol, 1 eq), 4-methylphosphonium pyridinium dichloride **2** (331 mg, 0.776 mmol, 4 eq), potassium *tert*-butoxide (261 mg, 2.325 mmol, 12 eq) and dry THF (30 mL). Reaction time: 14 hours. Purification: Column chromatography (Silica gel, Hexane:$CH_2Cl_2$:$Et_3N$ 48:48:3 and then $CH_2Cl_2$/MeOH 97:3) and gel permeation chromatography (Biobeads X1, Toluene) to obtain **3b** as a dark red solid with (146 mg, 81%). M.P.: 114-115 °C. FT-IR (KBr) ν/cm$^{-1}$: 3065, 3026, 2926, 2856, 1728, 1589, 1458, 1404, 1303, 1265, 1172, 1126, 940, 832, 793. $^1$H-NMR (400 MHz,

$CD_2Cl_2$) δ/ppm: 8.51 (d, 4H, $^3J$=6.0), 7.46 (d, 2H, $^3J$=16.0), 7,31 (d, 4H, $^3J$=6.0), 7.05 (s, 4H), 6.93 (s, 2H), 6.79 (d, 2H, $^3J$=16.0), 1.87 (m, 8H), 1.26 (m, 32H), 0.83 (t, 12H, $^3J$=6.8 Hz). $^{13}$C-NMR (100 MHz, $CD_2Cl_2$) δ/ppm: 160.5, 159.5, 150.7, 145.1, 145.0, 143.0, 138.5, 136.1, 127.5, 123.4, 123.3, 121.2 (two peaks), 120.8, 54.5, 38.3, 32.2, 30.3, 25.1, 23.2, 14.4. MS (MALDI-TOF) *m/z*: calculated for $C_{58}H_{70}N_2S_4$: 922.442; found: 923.020[M+]. UV-Vis ($CH_2Cl_2$) $\lambda_{max}$/nm (log ε): 528 (4.89).

**Synthesis of Py3CPDTV (3c).** According to the general procedure for Wittig reaction, using bisaldehyde **1c**[6] (219 mg, 0.191 mmol, 1 eq), 4-methylphosphonium pyridinium dichloride **2** (651 mg, 1.53 mmol, 8 eq), potassium *tert*-butoxide (386 mg, 3.44 mmol, 18 eq) and dry THF (30 mL). Reaction time: 16 hours. Purification: Column chromatography (Silica gel, Hexane:$CH_2Cl_2$:$Et_3N$ 48:48:3 and then $CH_2Cl_2$/MeOH 97:3) and gel permeation chromatography (Biobeads X1, Toluene) to obtain **3c** as a blue navy solid with (190 mg, 77%). M.P.: 136-137 °C. FT-IR (KBr) ν/cm$^{-1}$: 3065, 3019, 2926, 2856, 1720, 1589, 1458, 1411, 1303, 1265, 1180, 1126, 940, 832, 793. $^1$H-NMR (400 MHz, $CD_2Cl_2$) δ/ppm: 8.51 (d, 4H, $^3J$=6.0), 7.46 (d, 2H, $^3J$=16.0), 7,31 (d, 4H, $^3J$=6.0), 7.04 (s, 6H), 6.92 (s, 4H), 6.79 (d, 2H, $^3J$=16.0), 1.85 (m, 12H), 1.19 (m, 48H), 0.82 (m, 18H). $^{13}$C-NMR (100 MHz, $CD_2Cl_2$) δ/ppm: 160.5, 159.8, 159.4, 150.6, 145.2, 145.0, 144.2, 142.8, 138.5, 136.5, 135.8, 127.5, 123.4, 123.2, 121.4, 121.3, 121.0, 120.8, 120.7, 54.5, 38.3, 32.2, 30.2, 25.1, 23.2, 14.4. MS (MALDI-TOF) *m/z*: calculated for $C_{81}H_{100}N_2S_6$: 1292.621; found: 1293.431[M+]. UV-Vis ($CH_2Cl_2$) $\lambda_{max}$/nm (log ε): 564 (5.02).

**Synthesis of Py4CPDTV (3d).** According to the general procedure for Wittig reaction, using bisaldehyde **1d**[6] (114 mg, 0.075 mmol, 1 eq), 4-methylphosphonium pyridinium dichloride **2** (256 mg, 0.6 mmol, 8 eq), potassium *tert*-butoxide (152 mg, 1.35 mmol, 18 eq) and dry THF (14 mL). Reaction time: 24 hours. Purification: Column chromatography (Silica gel, Hexane:$CH_2Cl_2$:$Et_3N$ 48:48:3 and then $CH_2Cl_2$/MeOH 96:4) and gel permeation chromatography (Biobeads X1, Toluene) to obtain **3d** as a dark purple solid with (80 mg, 64%). M.p.: 166-167 °C. FT-IR (KBr) ν/cm$^{-1}$: 3065, 3019, 2926, 2856, 1720, 1589, 1489, 1404, 1272, 1180, 1126, 1079, 963, 824. $^1$H-NMR (400 MHz, $CD_2Cl_2$) δ/ppm: 8.50 (d, 4H, $^3J$=6.0), 7.45 (d, 2H, $^3J$=16.0), 7,29 (d, 4H, $^3J$=6.0), 7.02 (m, 8H), 6.90 (m, 4H), 6.76 (d, 2H, $^3J$=16.0), 1.83 (m, 16H), 1.24 (m, 63H), 0.85 (m, 24H). $^{13}$C-NMR (100 MHz, $CD_2Cl_2$) δ/ppm : 160.4, 159.8, 159.6, 159.3, 150.6, 145.3, 144.9, 144.5, 144.2, 142.8, 138.6, 136.6, 136.3, 135.8, 127.4, 125.3, 124.5, 123.3, 123.2, 121.4, 121.3, 121.0, 120.9, 120.7, 120.6, 54.4, 38.3, 32.2, 30.8, 25.1, 23.2, 14.4. MS (MALDI-TOF) *m/z*: calculated for $C_{104}H_{130}N_2S_8$: 1663.803; found: 1663.848[M+]. UV-Vis ($CH_2Cl_2$) $\lambda_{max}$/nm (log ε): 588 (4.88).

## Part 3. Characterization: NMR Spectra, FT-IR Spectra and MS (MALDI-TOF) Spectra

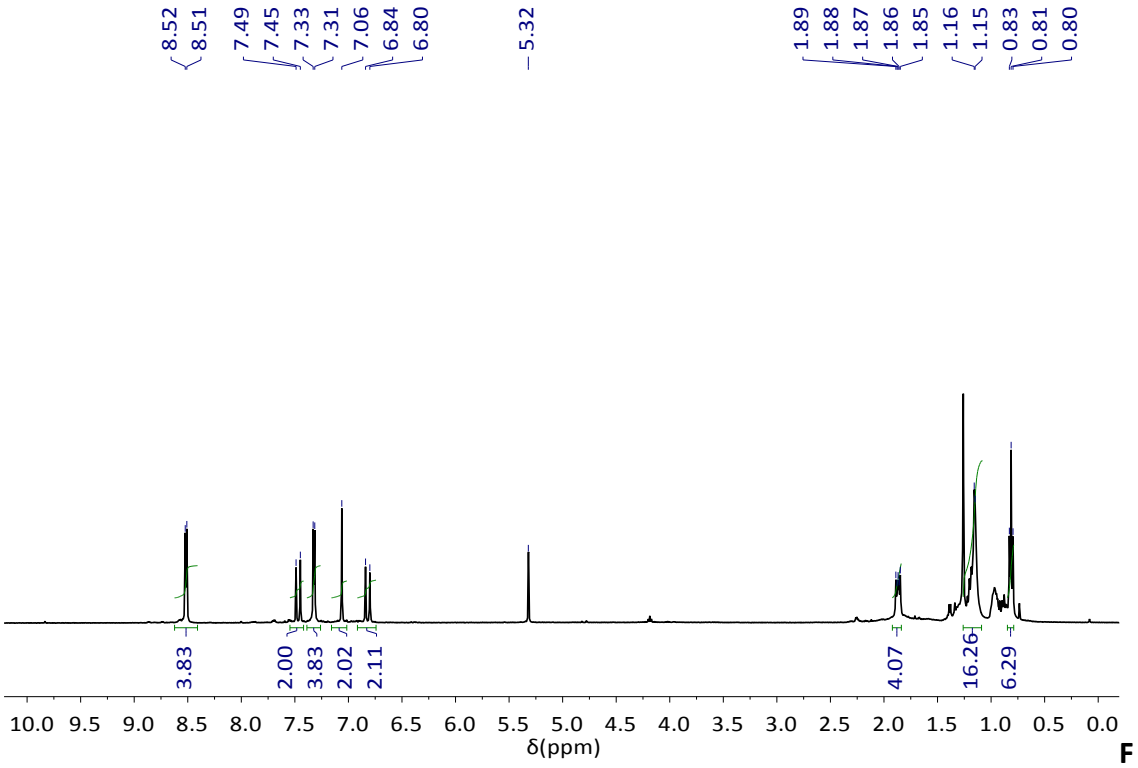


**igure S1.** $^{1}$H NMR (400 MHz, $CD_2Cl_2$) spectrum of compound **Py1CPDTV (3a)**.

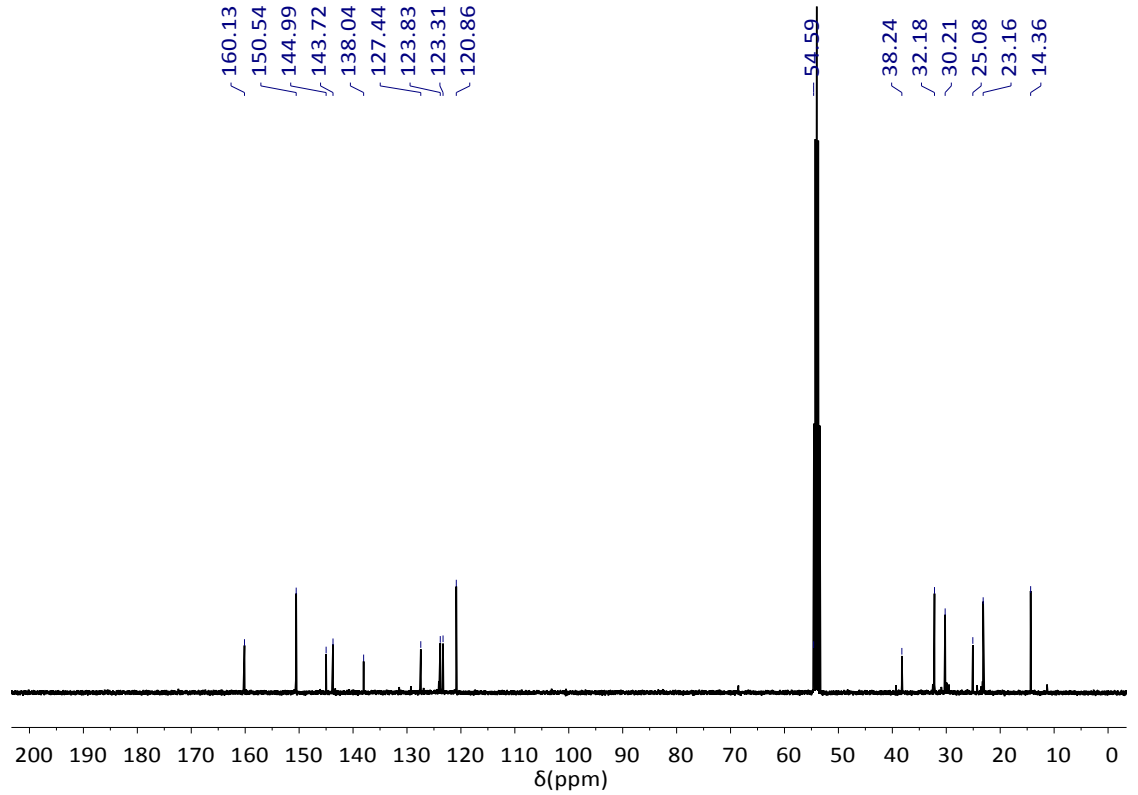


**Figure S2.** $^{13}$C NMR (100 MHz, $CD_2Cl_2$) spectrum of compound **Py1CPDTV (3a)**.

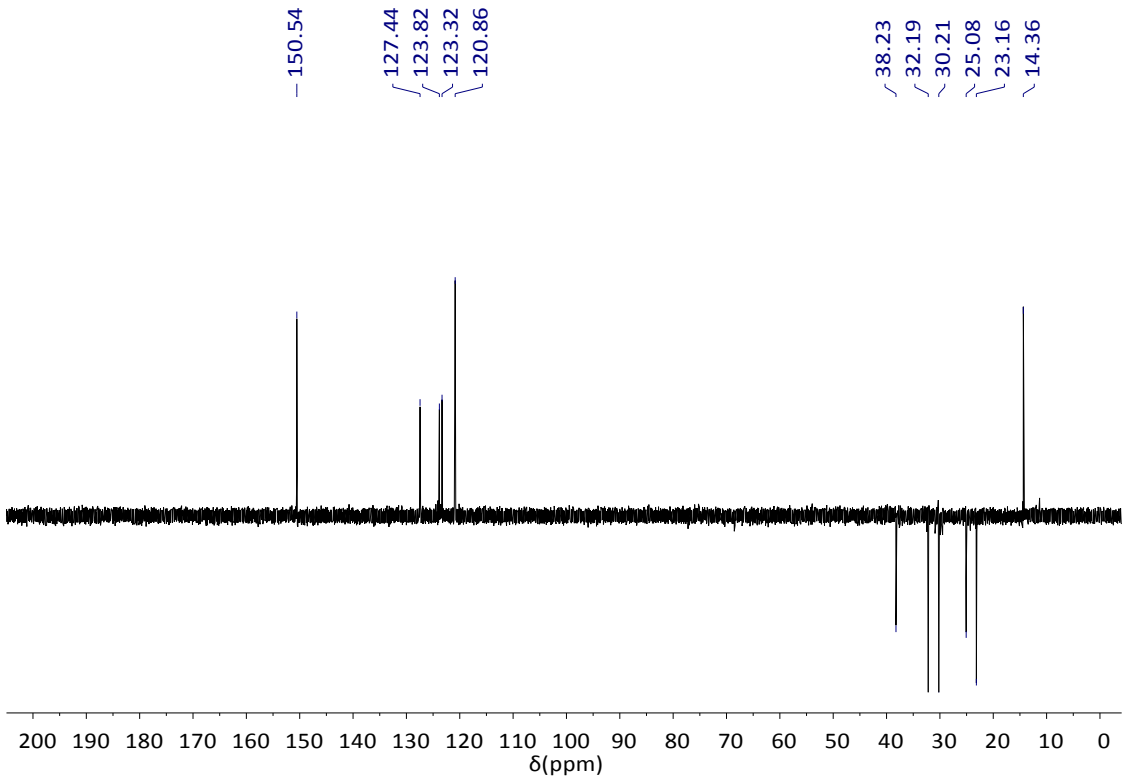


**Figure S3.** $^{13}C$ NMR DEPT135 (100 MHz, $CD_2Cl_2$) spectrum of compound **Py1CPDTV (3a)**.

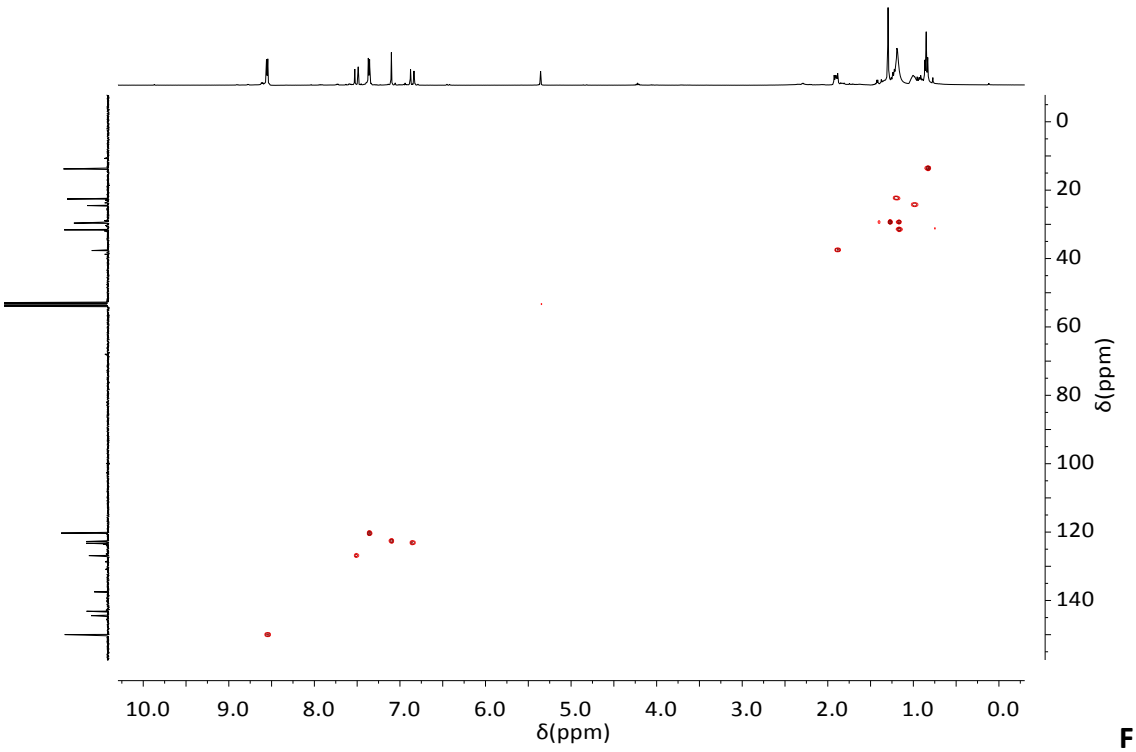


**Figure S4.** 2D $^{1}H$ $^{13}C$ HSQC NMR ($CD_2Cl_2$) spectrum of compound **Py1CPDTV (3a)**.

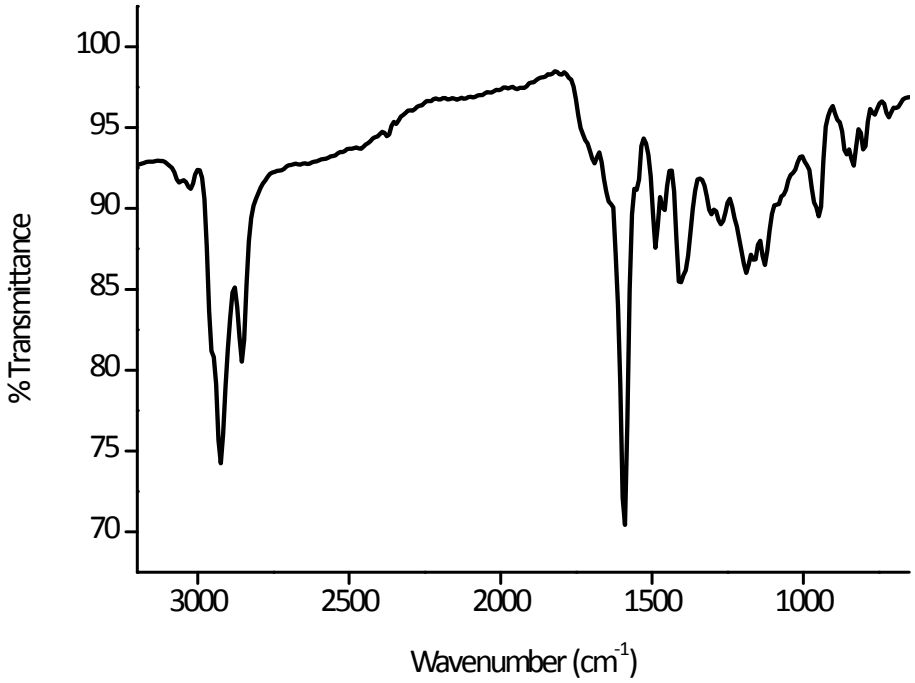


**Figure S5.** FT-IR (KBr) spectrum of compound **Py1CPDTV (3a)**.

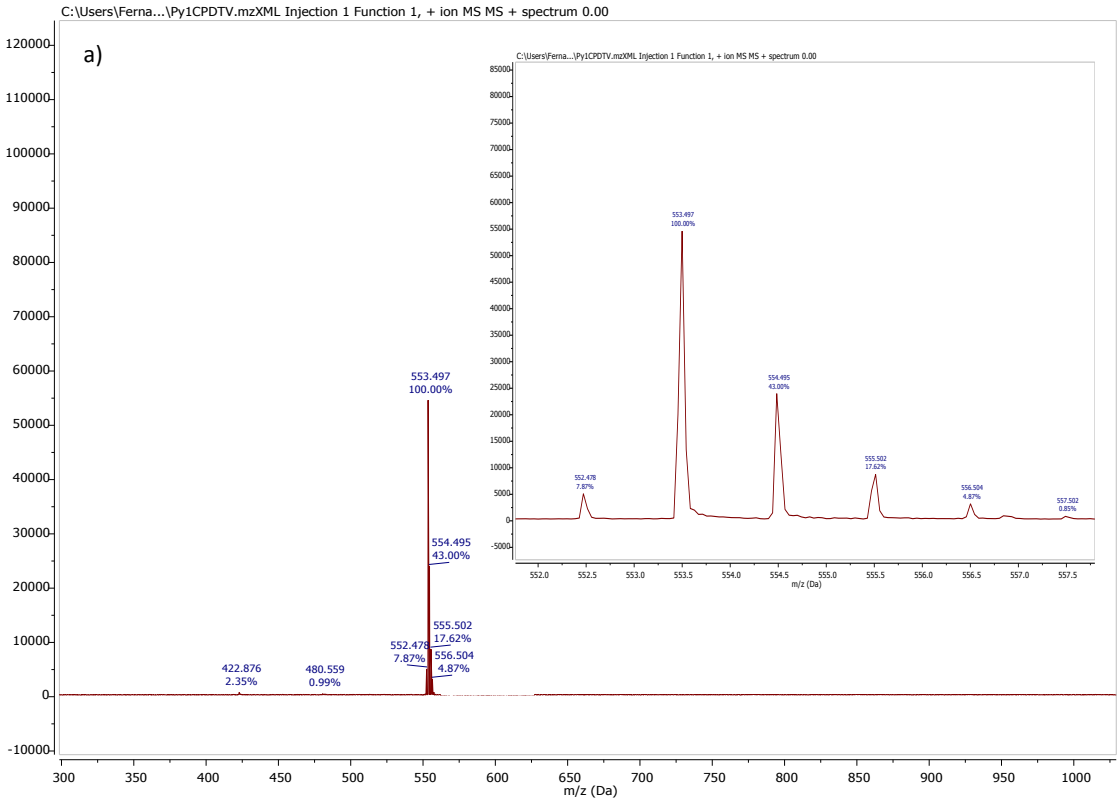

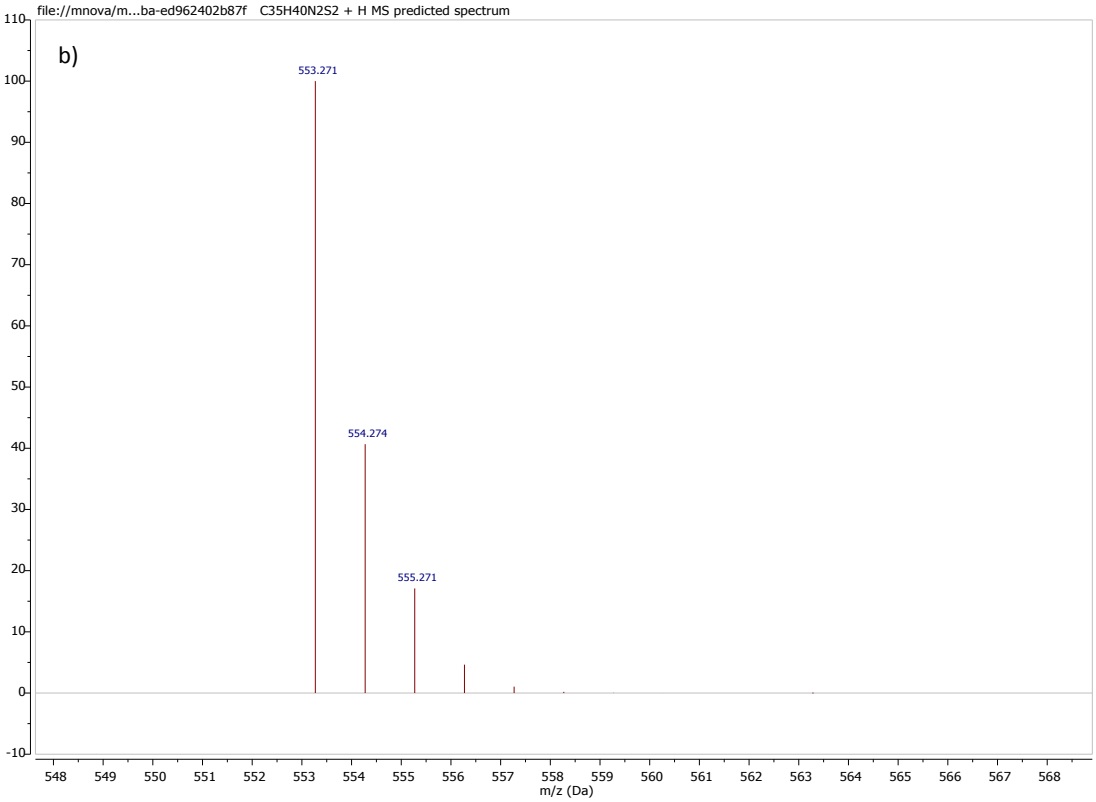


**Figure S6.** a) MS (MALDI-TOF) spectrum and isotopic distribution of compound **Py1CPDTV (3a)** and b) MS (MALDI-TOF) theoretical for compound **Py1CPDTV (3a)** [M+].

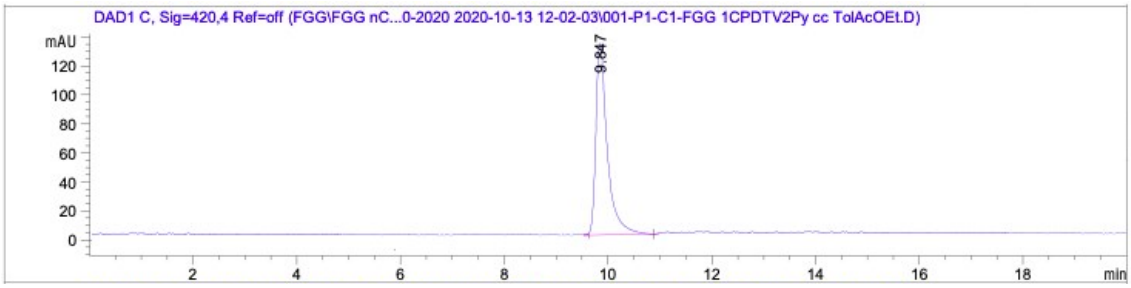


**Figure S7.** HPLC profile of compound **Py1CPDTV (3a)**. Conditions: HPLC column: Buckyprep (4.6ID x 250 mm)), Toluene/Ethyl Acetate (95:5) as eluent (1mL/min); λ=420 nm; 25 °C.

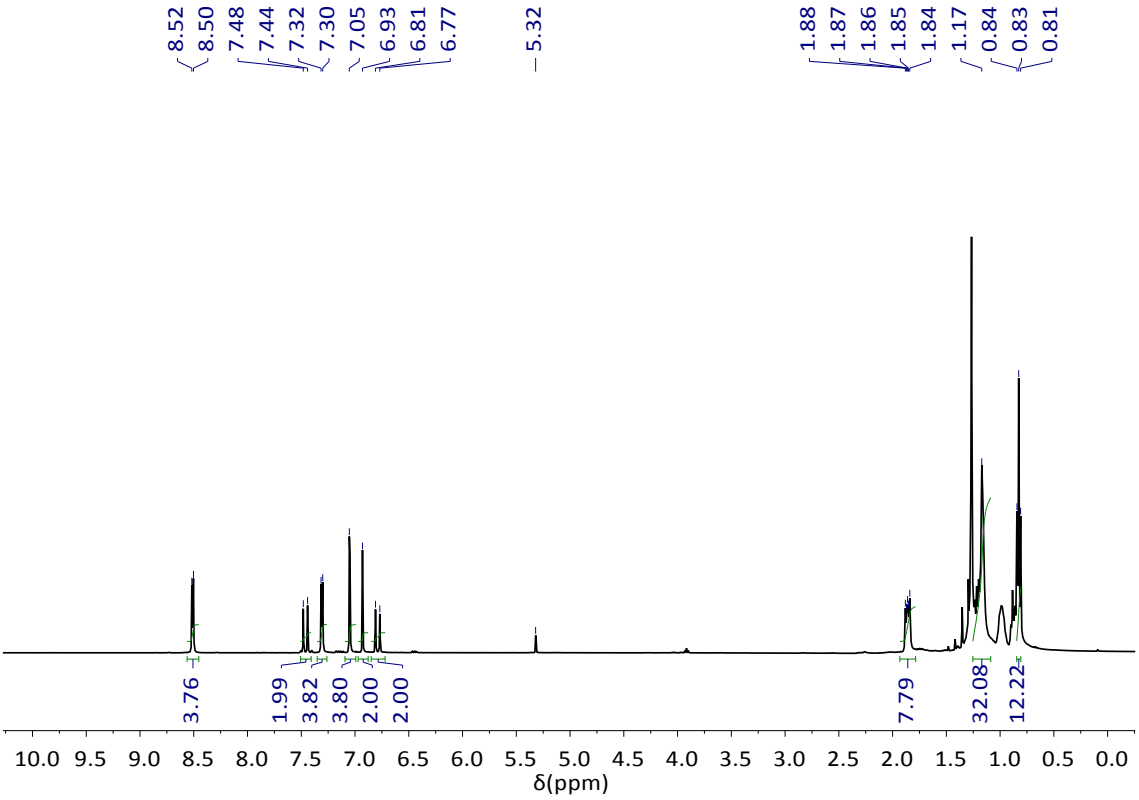


**Figure S8.** $^{1}H$ NMR (400 MHz, $CD_2Cl_2$) spectrum of compound **Py2CPDTV (3b)**.

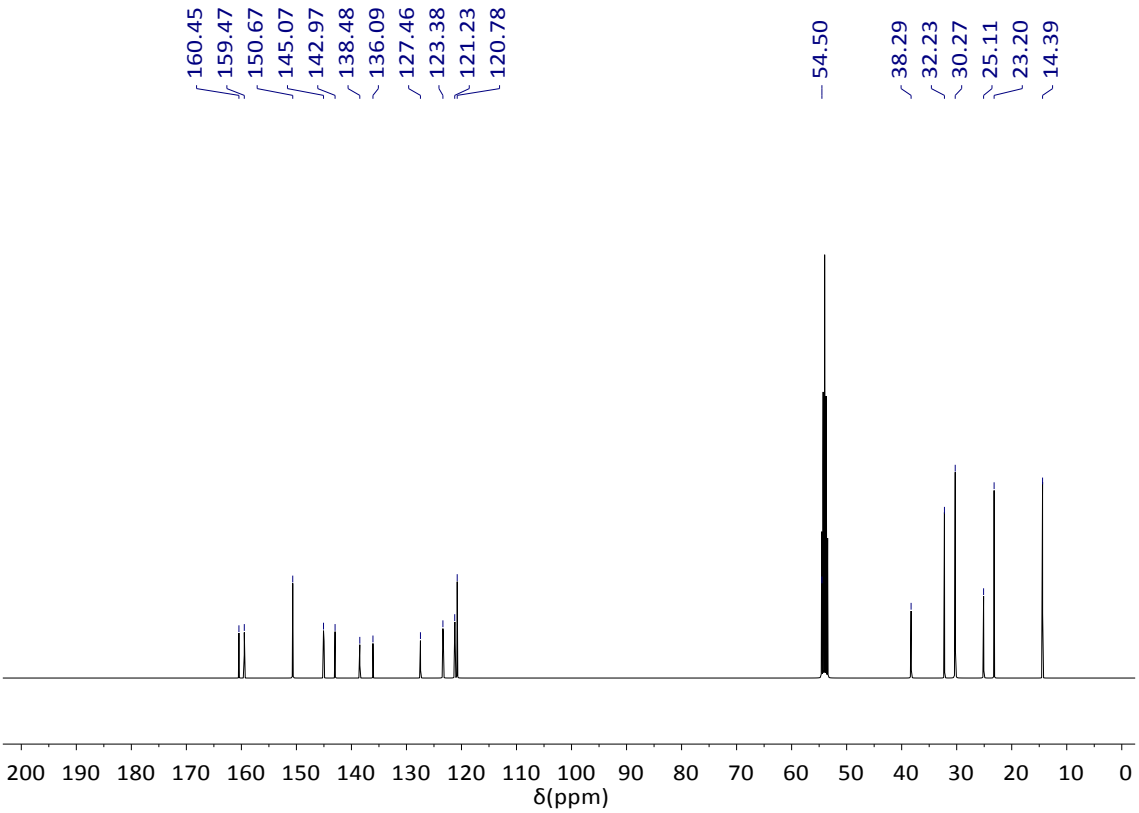


**Figure S9.** $^{13}C$ NMR (100 MHz, $CD_2Cl_2$) spectrum of compound **Py2CPDTV (3b).**

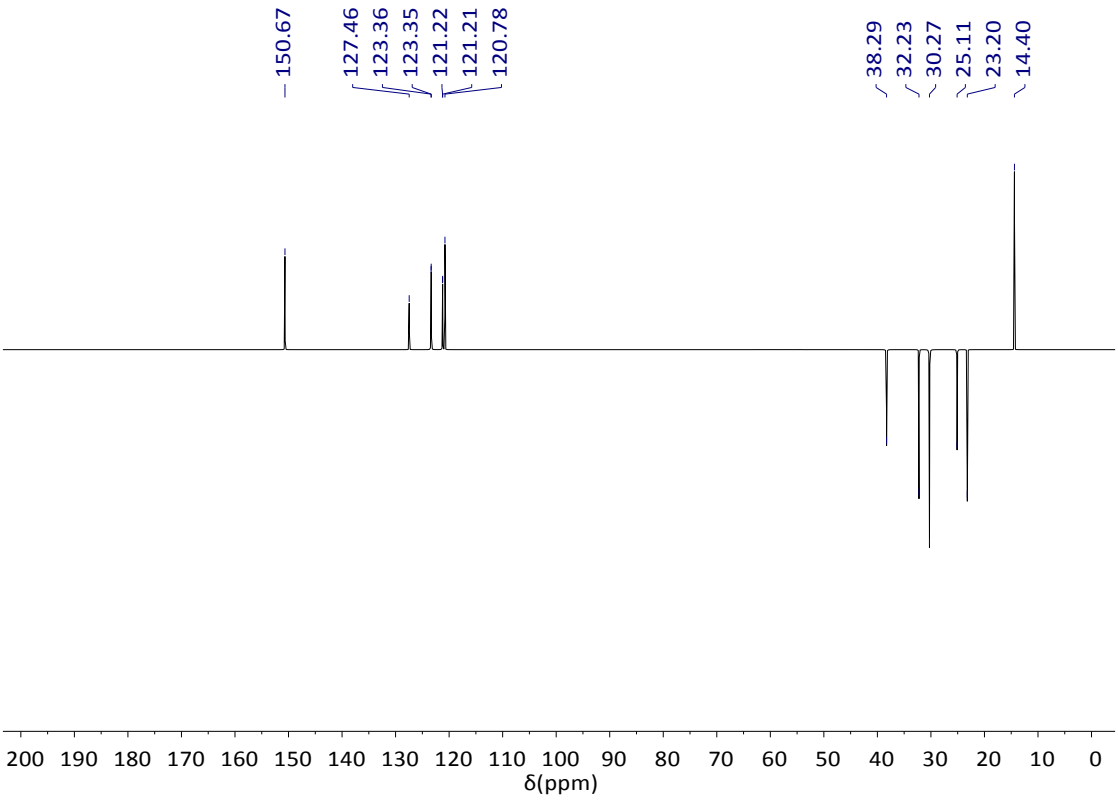


**Figure S10.** $^{13}C$ NMR DEPT135 (100 MHz, $CD_2Cl_2$) spectrum of compound **Py2CPDTV (3b)**.

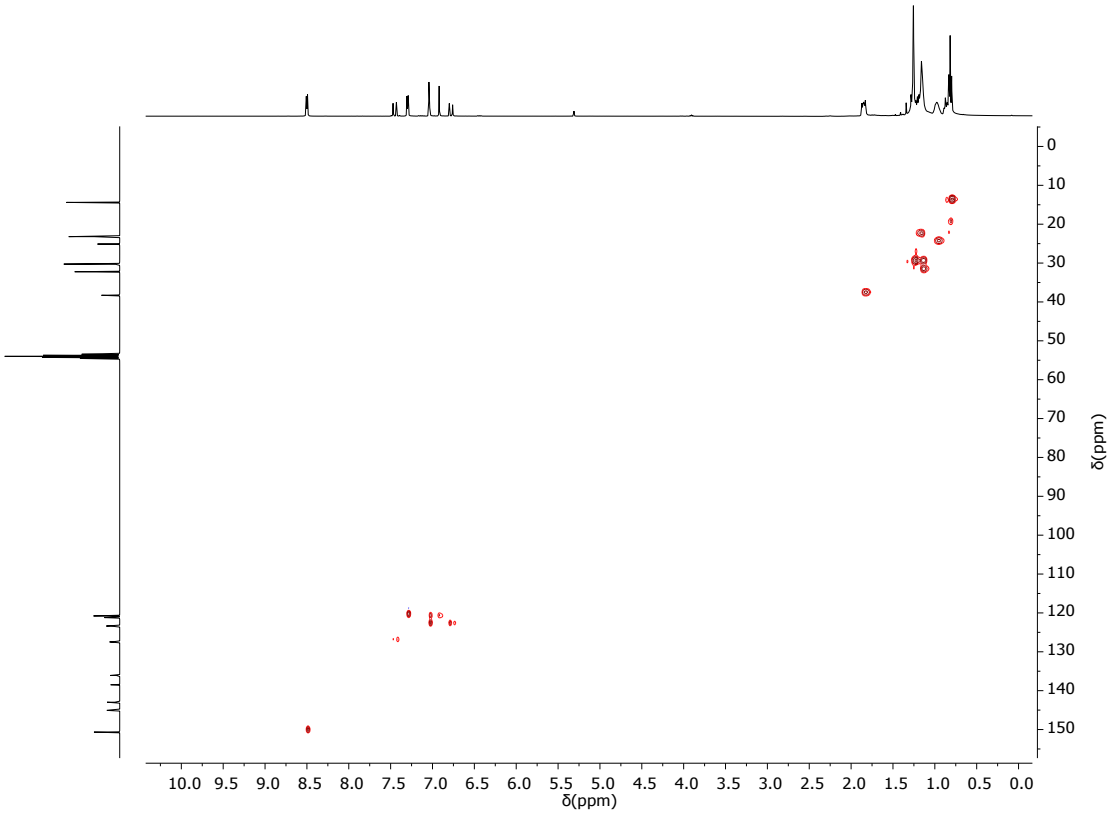


**Figure S11.** 2D $^{1}H$ $^{13}C$ HSQC NMR ($CD_2Cl_2$) spectrum of compound **Py2CPDTV (3b)**.

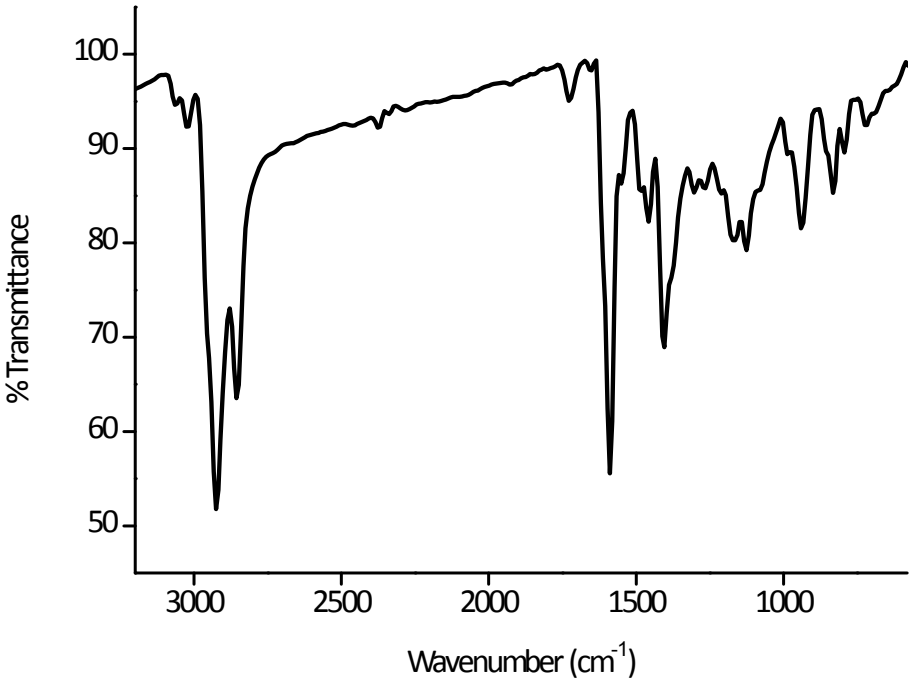


**Figure S12.** FT-IR (KBr) spectrum of compound **Py2CPDTV (3b)**.

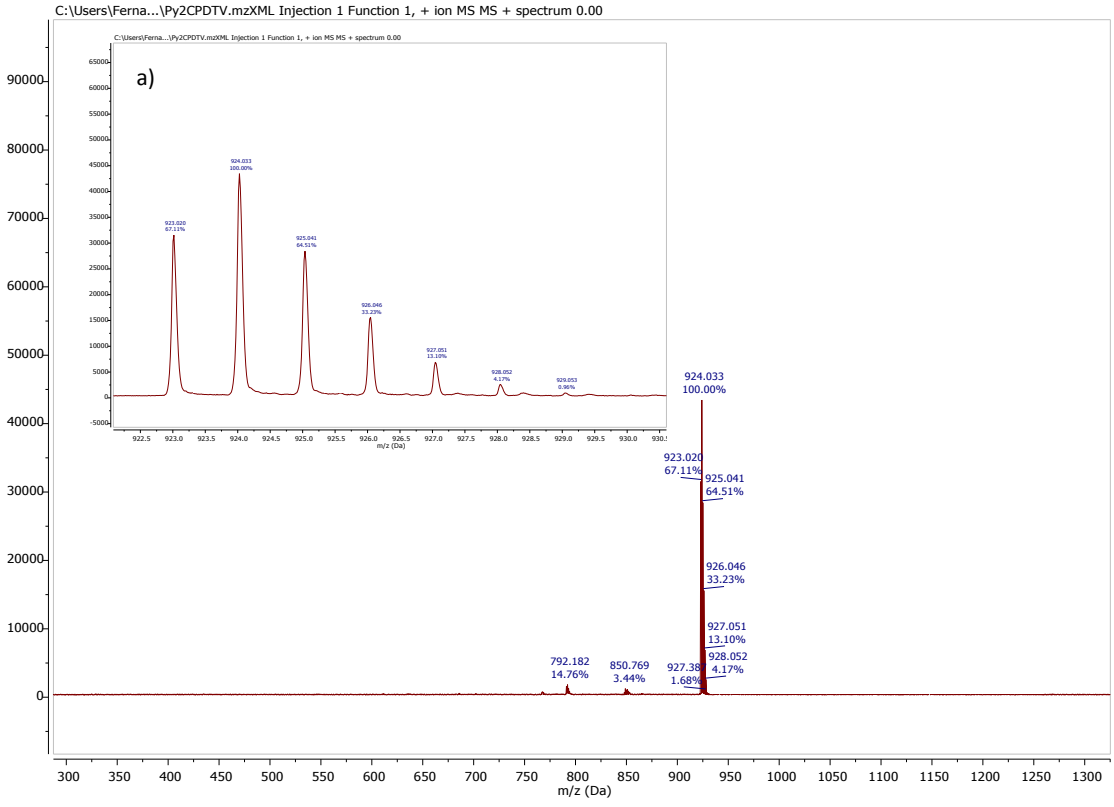

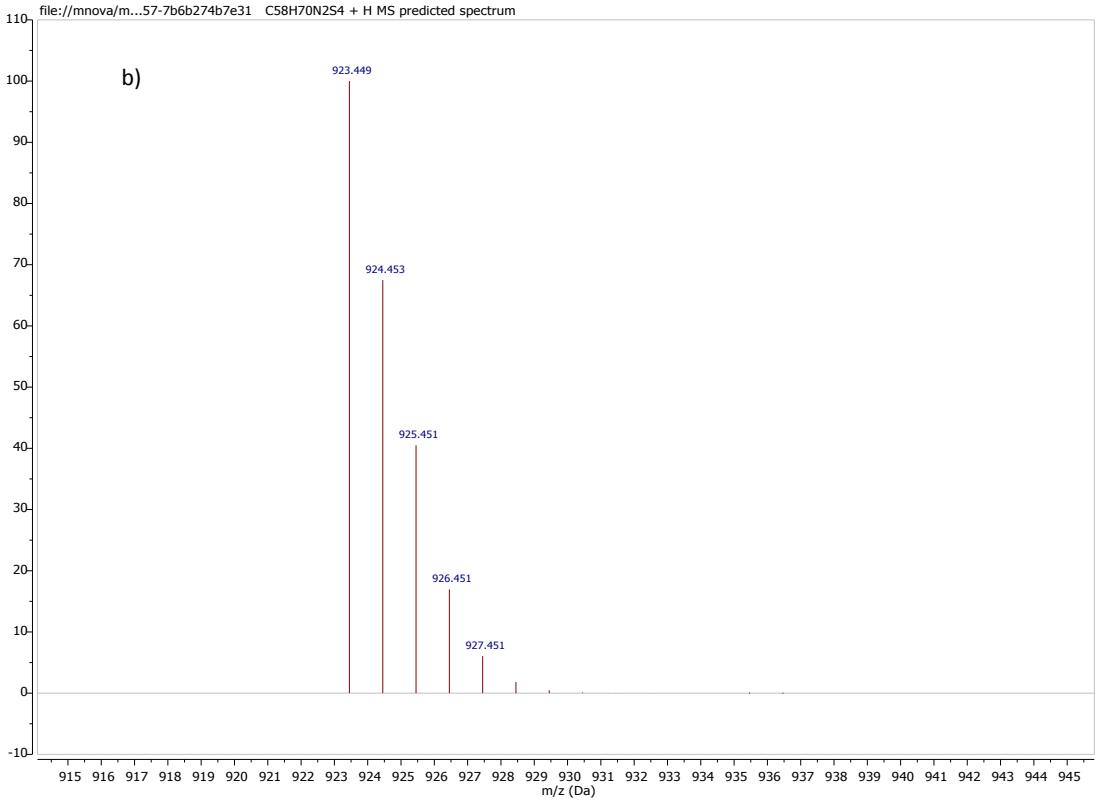


**Figure S13.** a) MS (MALDI-TOF) spectrum and isotopic distribution of compound **Py2CPDTV (3b)** and b) MS (MALDI-TOF) theoretical for compound **Py2CPDTV (3b)** [M+].

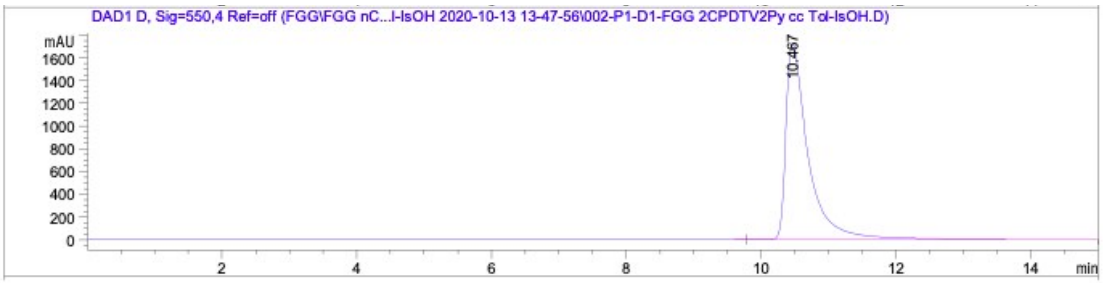


**Figure S14.** HPLC profile of compound **Py2CPDTV (3b)**. Conditions: HPLC column: Buckyprep (4.6ID x 250 mm)), Toluene/Isopropanol (98:2) as eluent (1mL/min); λ=550 nm; 25 °C.

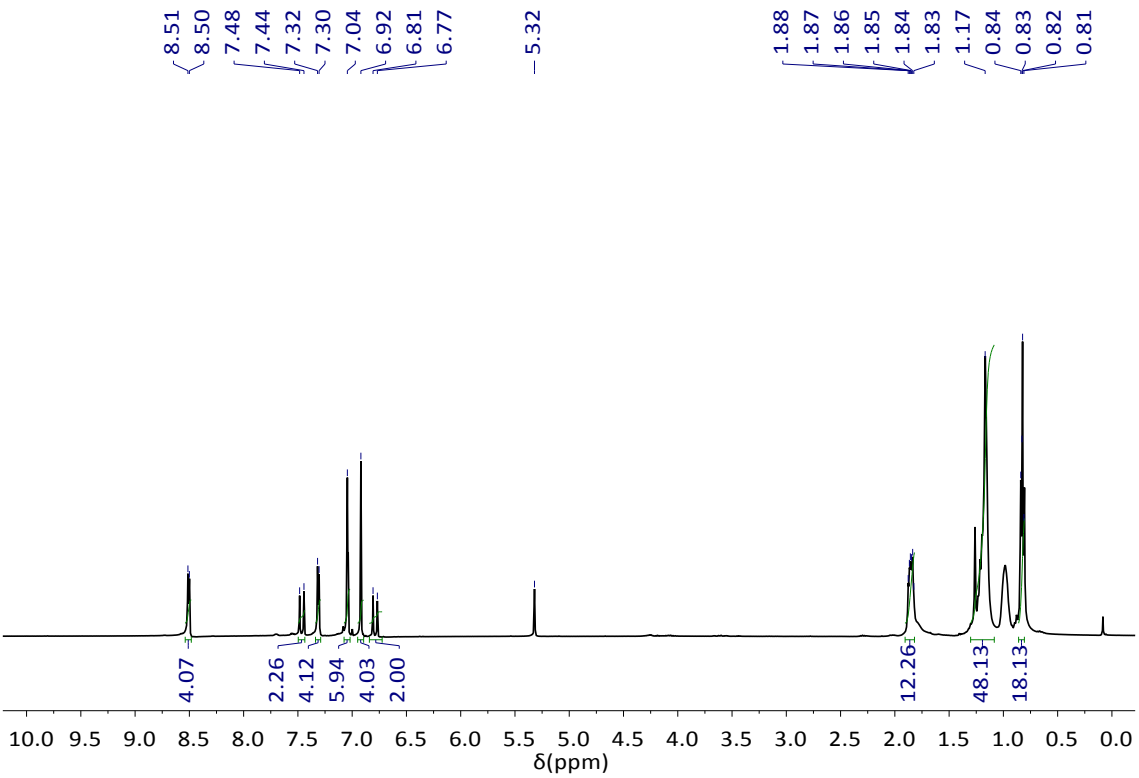


**Figure S15.** $^{1}H$ NMR (400 MHz, $CD_2Cl_2$) spectrum of compound **Py3CPDTV (3c)**.

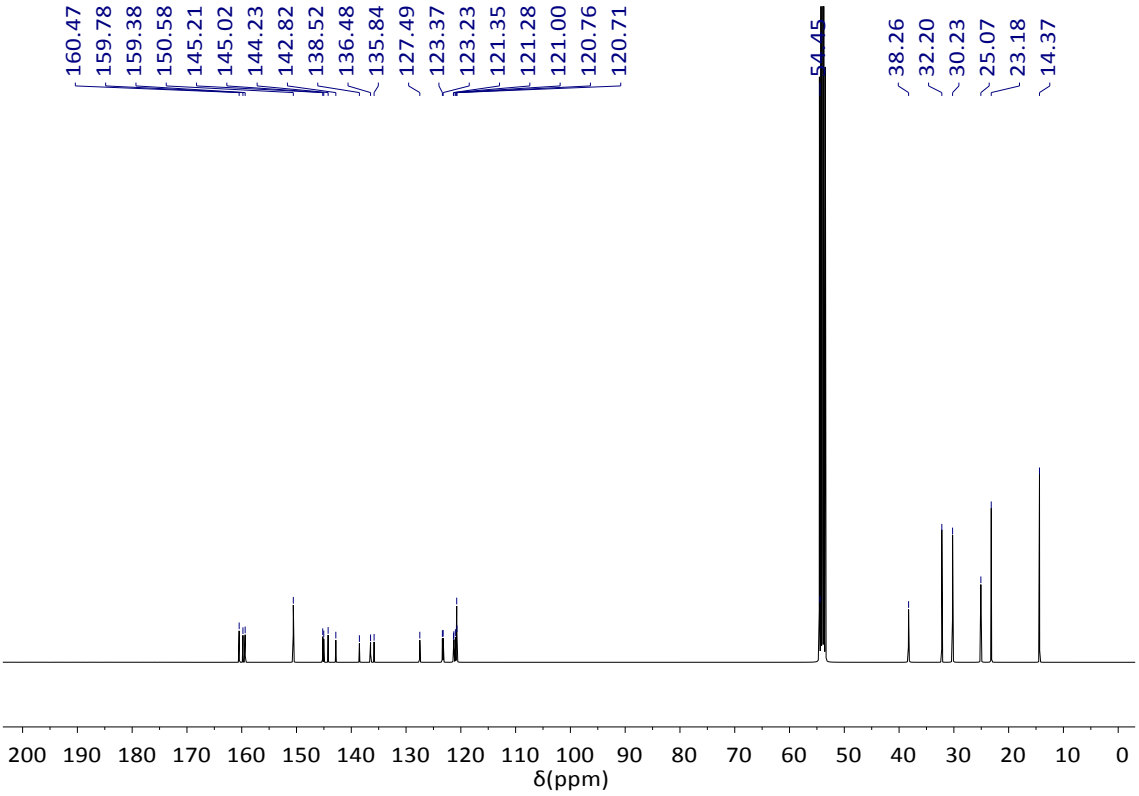


**Figure S16.** $^{13}C$ NMR (100 MHz, $CD_2Cl_2$) spectrum of compound **Py3CPDTV (3c)**.

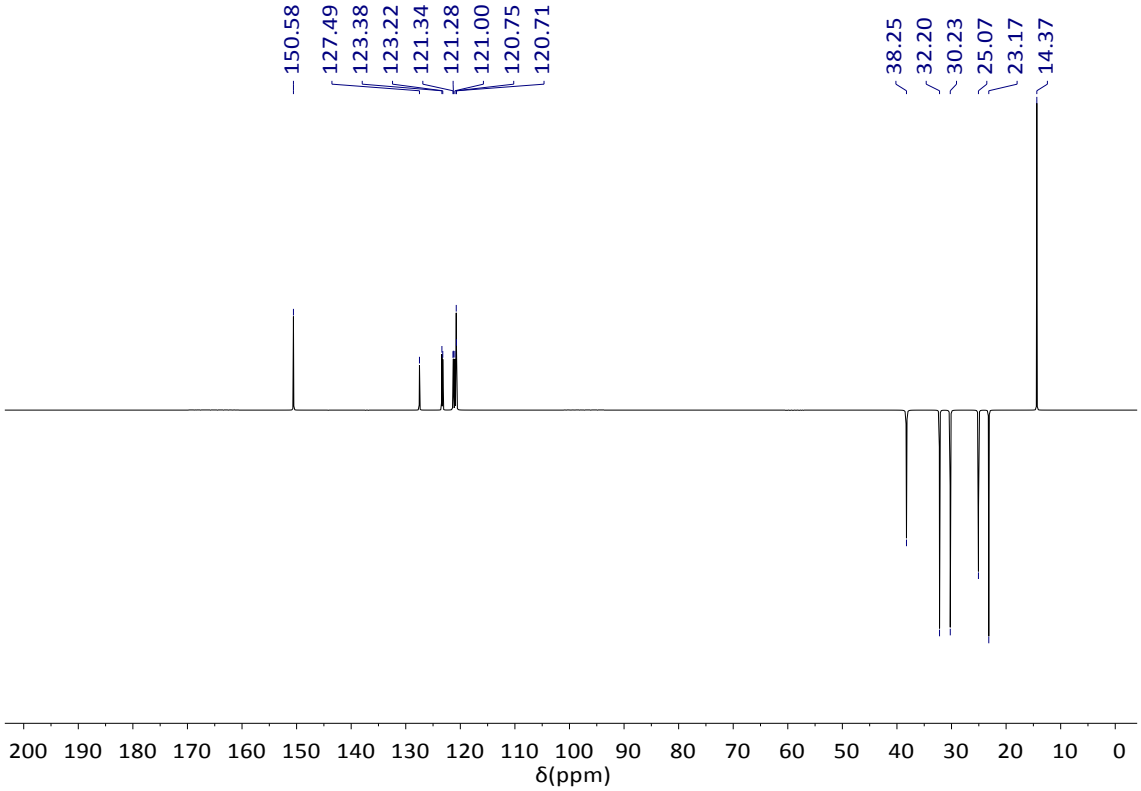


**Figure S17.** $^{13}C$ NMR DEPT135 (100 MHz, $CD_2Cl_2$) spectrum of compound **Py3CPDTV (3c)**.

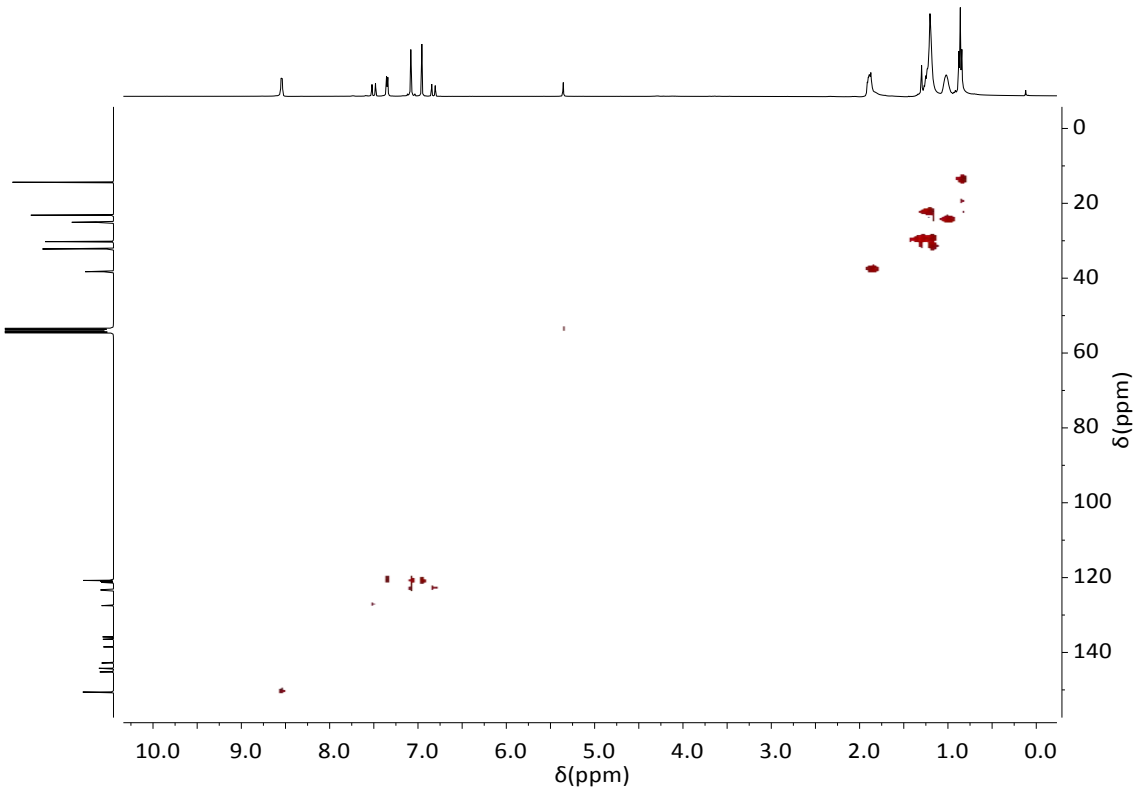


**Figure S18.** 2D $^{1}H$ $^{13}C$ HSQC NMR ($CD_2Cl_2$) spectrum of compound **Py3CPDTV (3c)**.

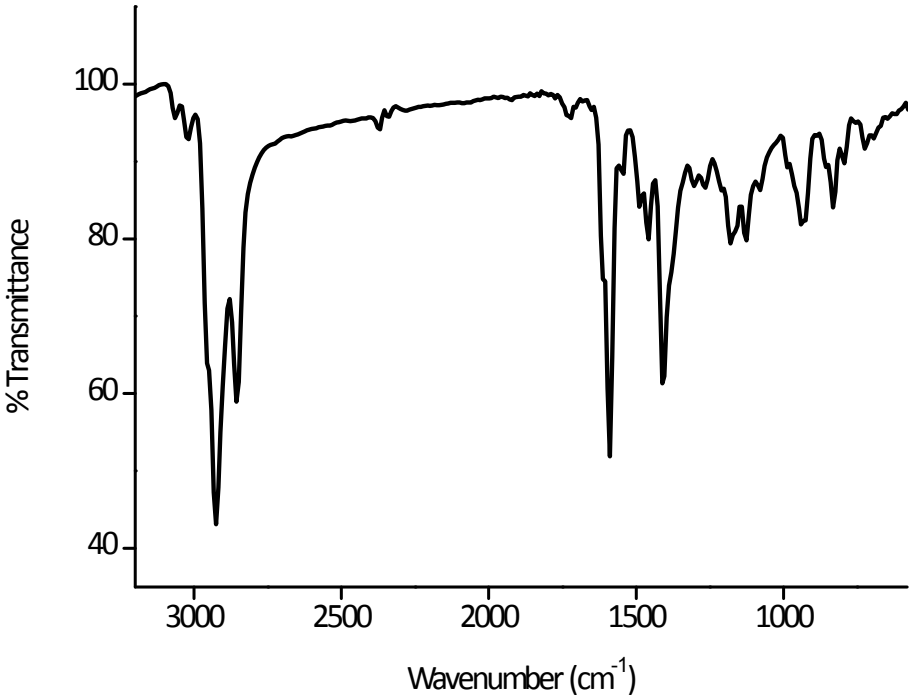


**Figure S19.** FT-IR (KBr) spectrum of compound **Py3CPDTV (3c)**.

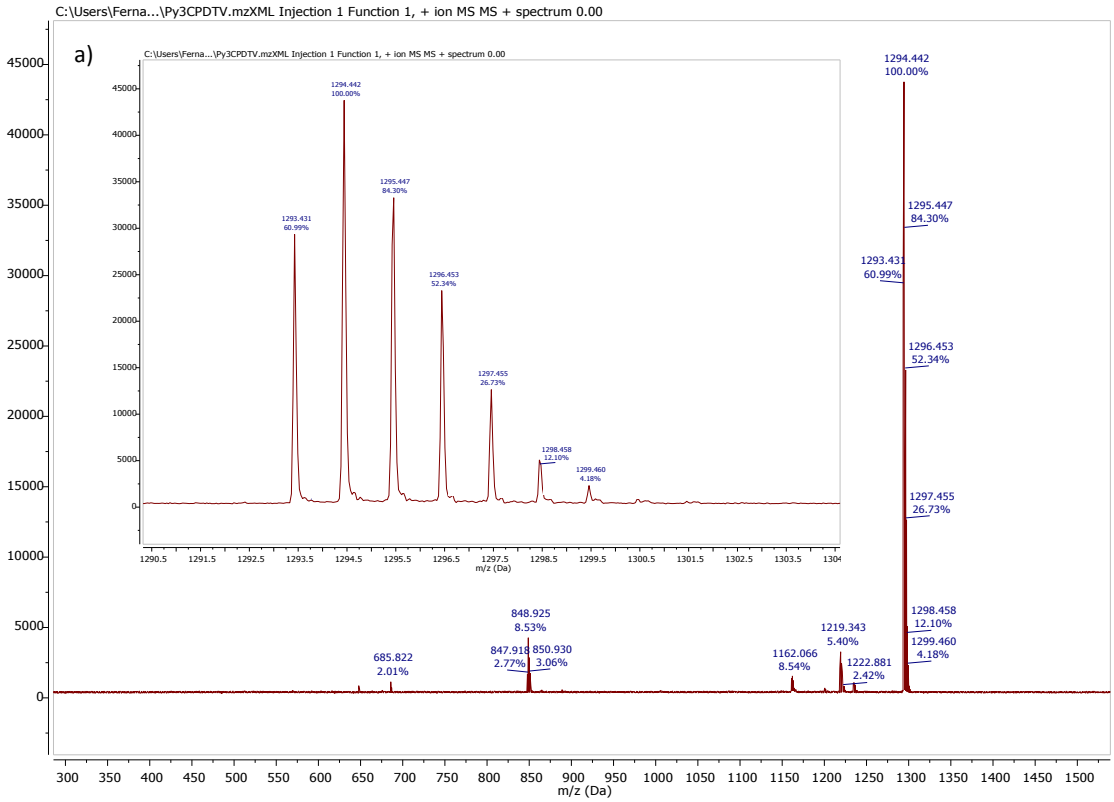

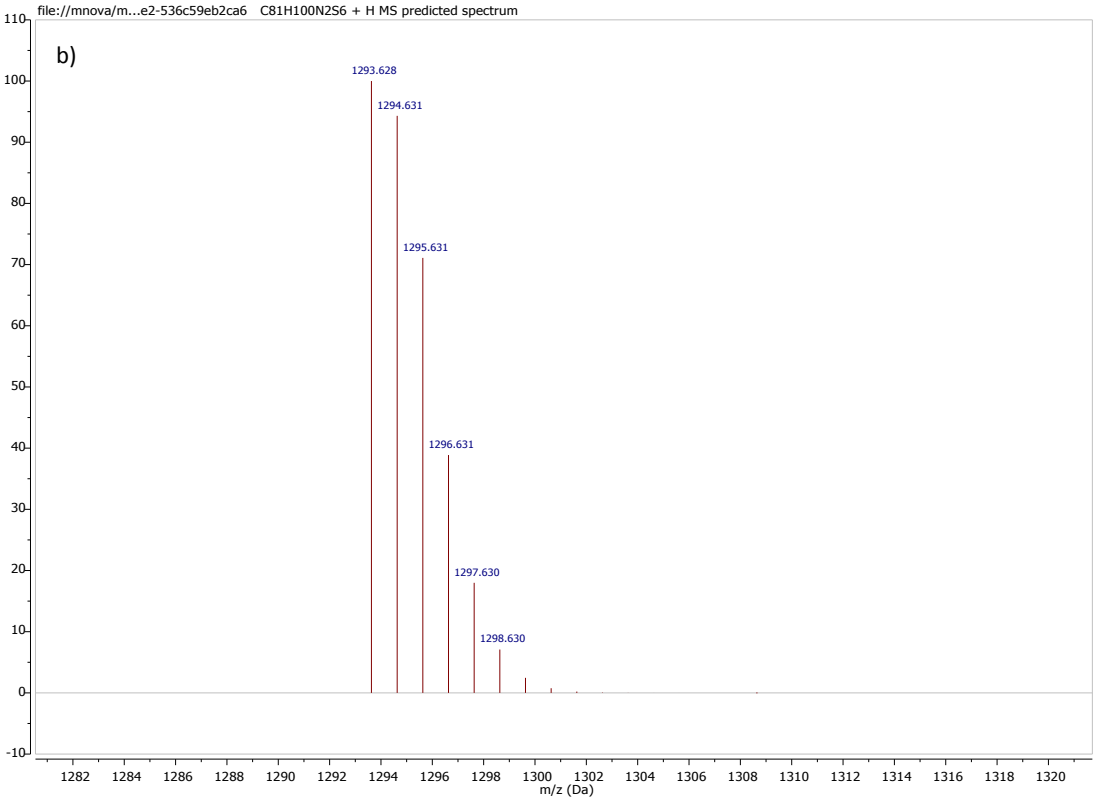


**Figure S20.** a) MS (MALDI-TOF) spectrum and isotopic distribution of compound **Py3CPDTV (3c)** and b) MS (MALDI-TOF) theoretical for compound **Py3CPDTV (3c)** [M+].

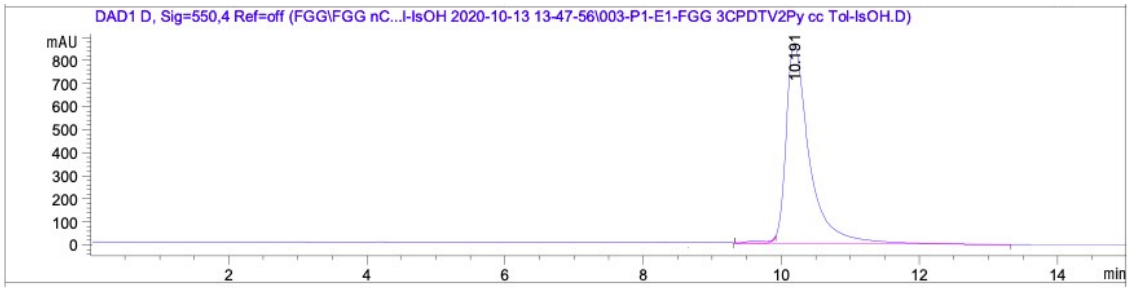


**Figure S21.** HPLC profile of compound **Py3CPDTV (3c)**. Conditions: HPLC column: Buckyprep (4.6ID x 250 mm)), Toluene/Isopropanol (98:2) as eluent (1mL/min); λ=550 nm; 25 °C.

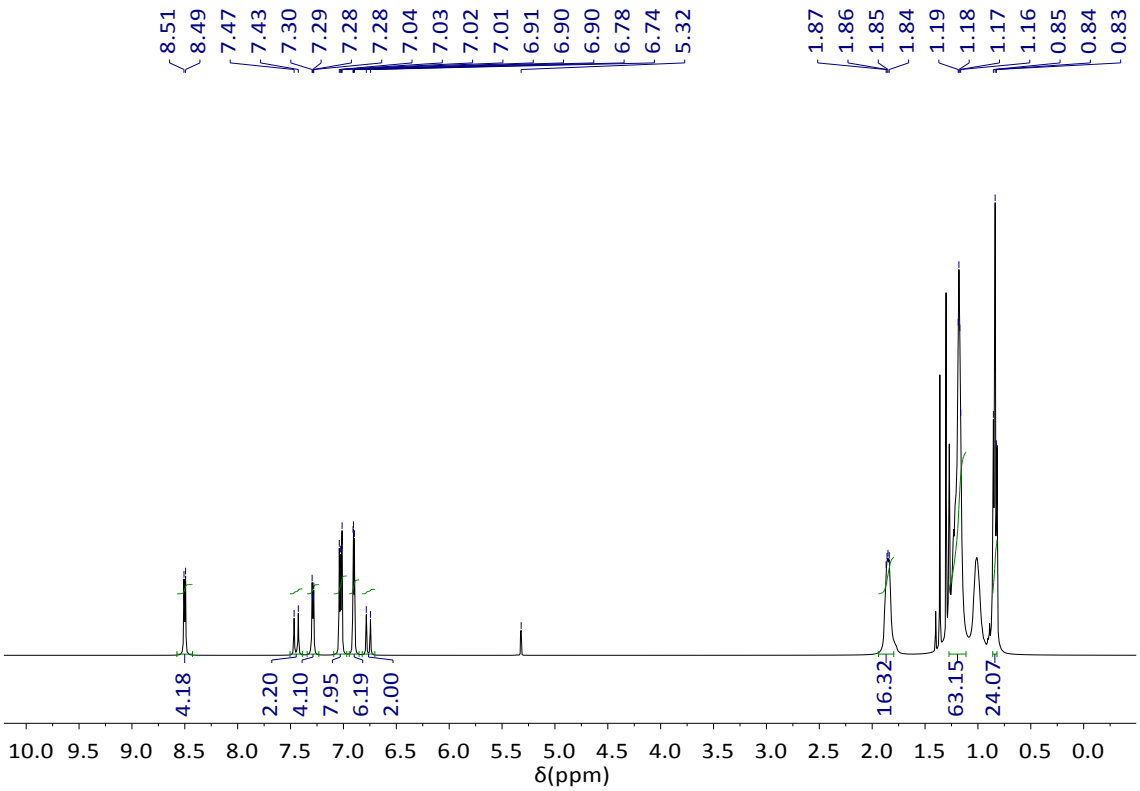


**Figure S22.** $^{1}$H NMR (400 MHz, $CD_2Cl_2$) spectrum of compound **Py4CPDTV (3d)**.

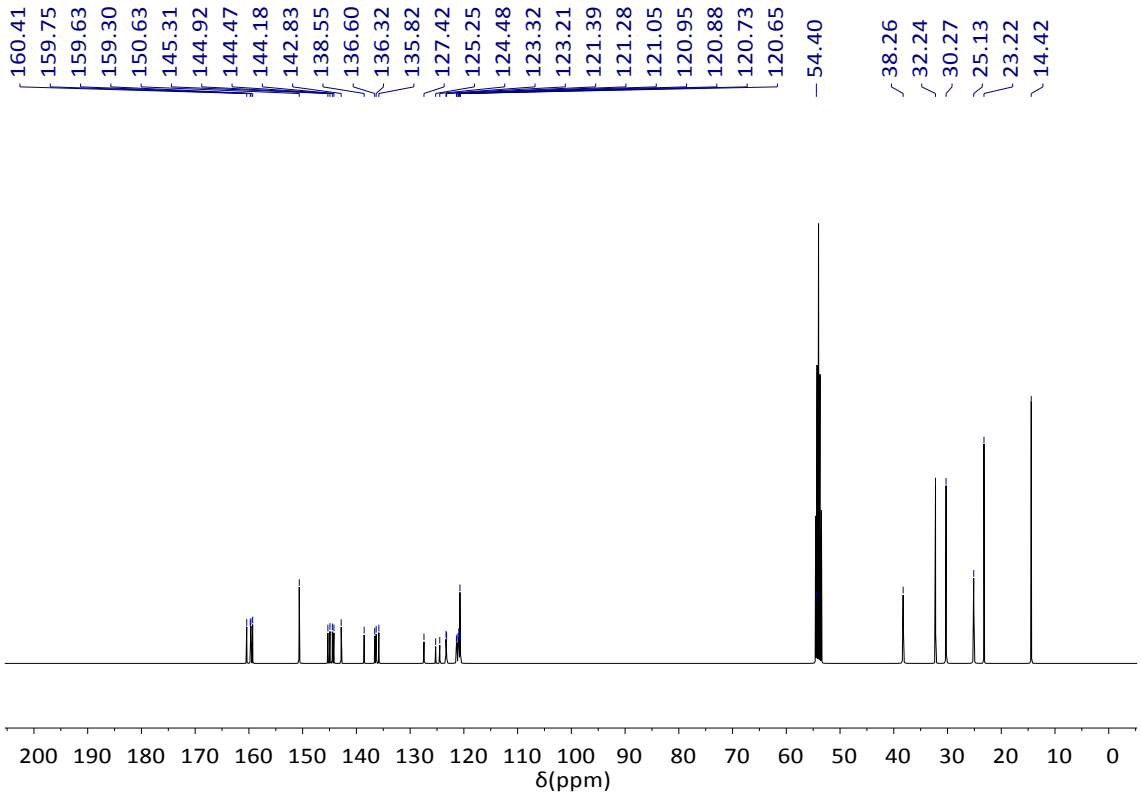


**Figure S23.** $^{13}$C NMR (100 MHz, $CD_2Cl_2$) spectrum of compound **Py4CPDTV (3d)**.

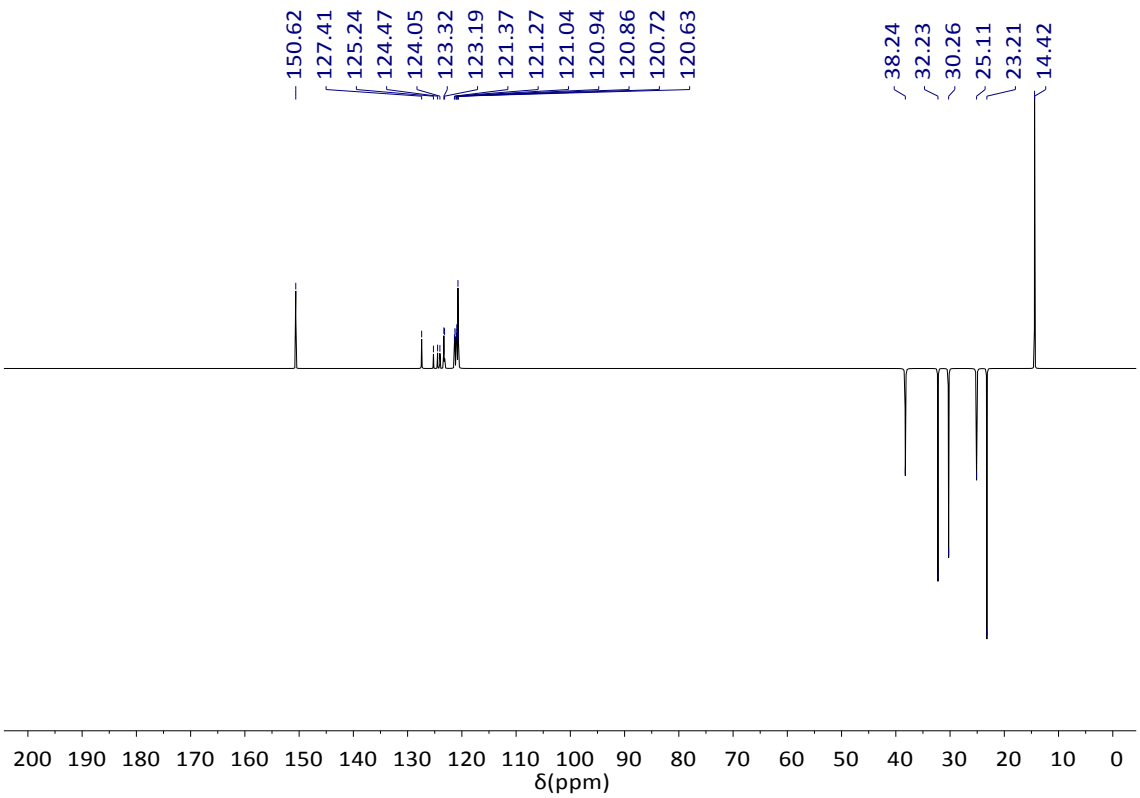


**Figure S24.** $^{13}C$ NMR DEPT135 (100 MHz, $CD_2Cl_2$) spectrum of compound **Py4CPDTV (3d)**.

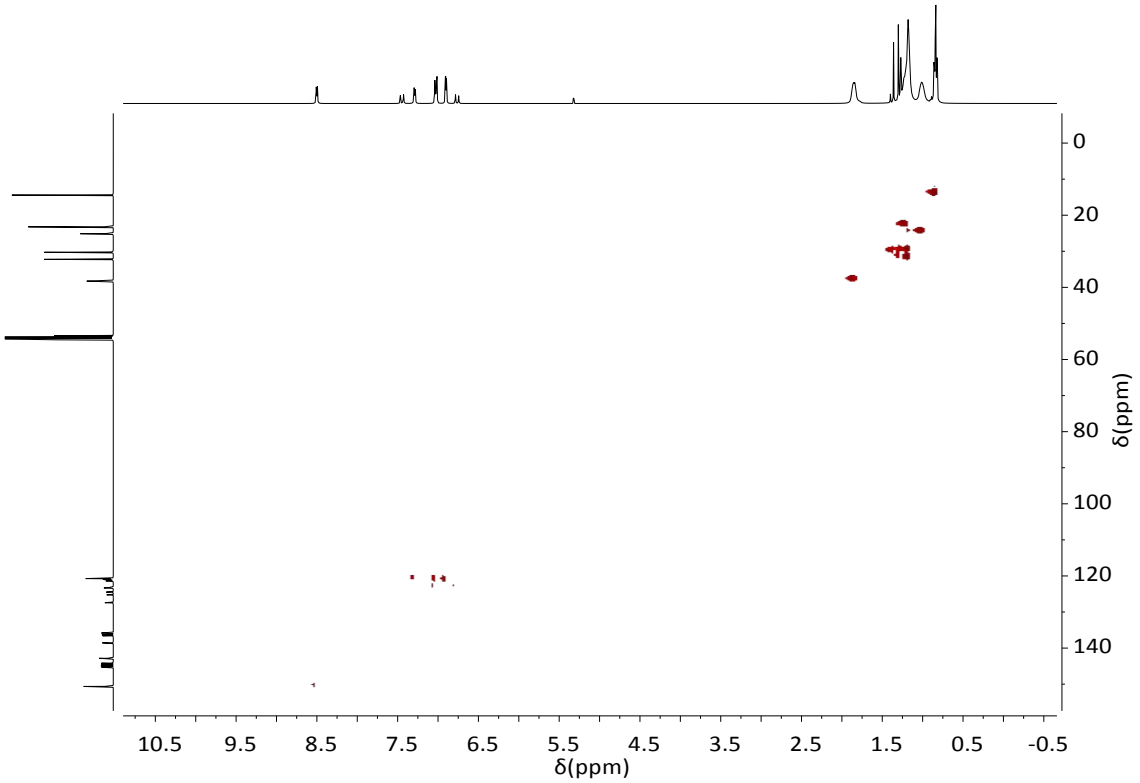


**Figure S25**. 2D $^{1}H$ $^{13}C$ HSQC NMR ($CD_2Cl_2$) spectrum of compound **Py4CPDTV (3d)**.

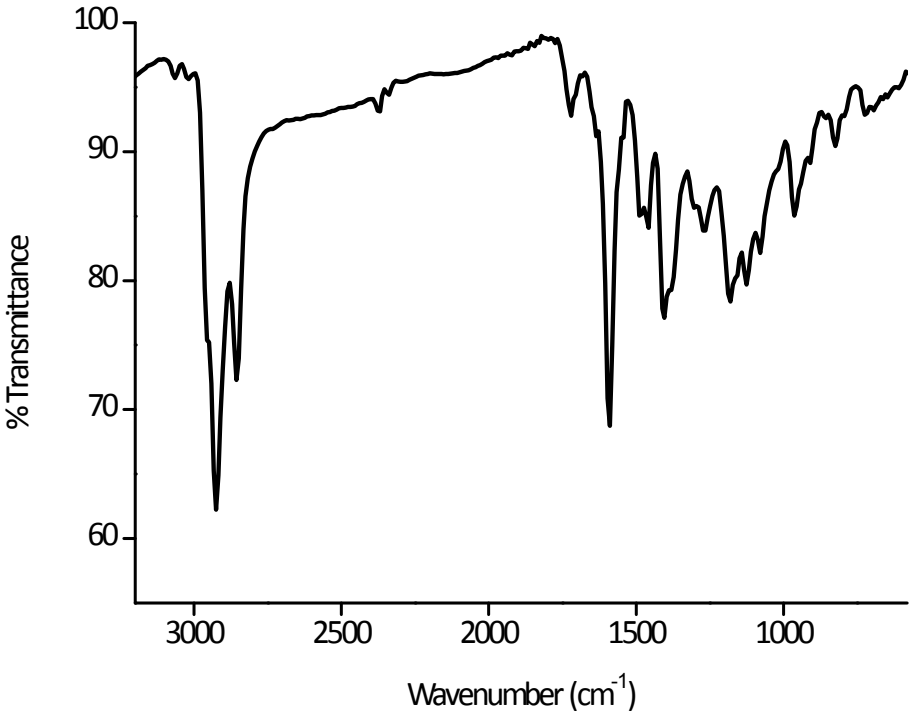


**Figure S26.** FT-IR (KBr) spectrum of compound **Py4CPDTV (3d)**.

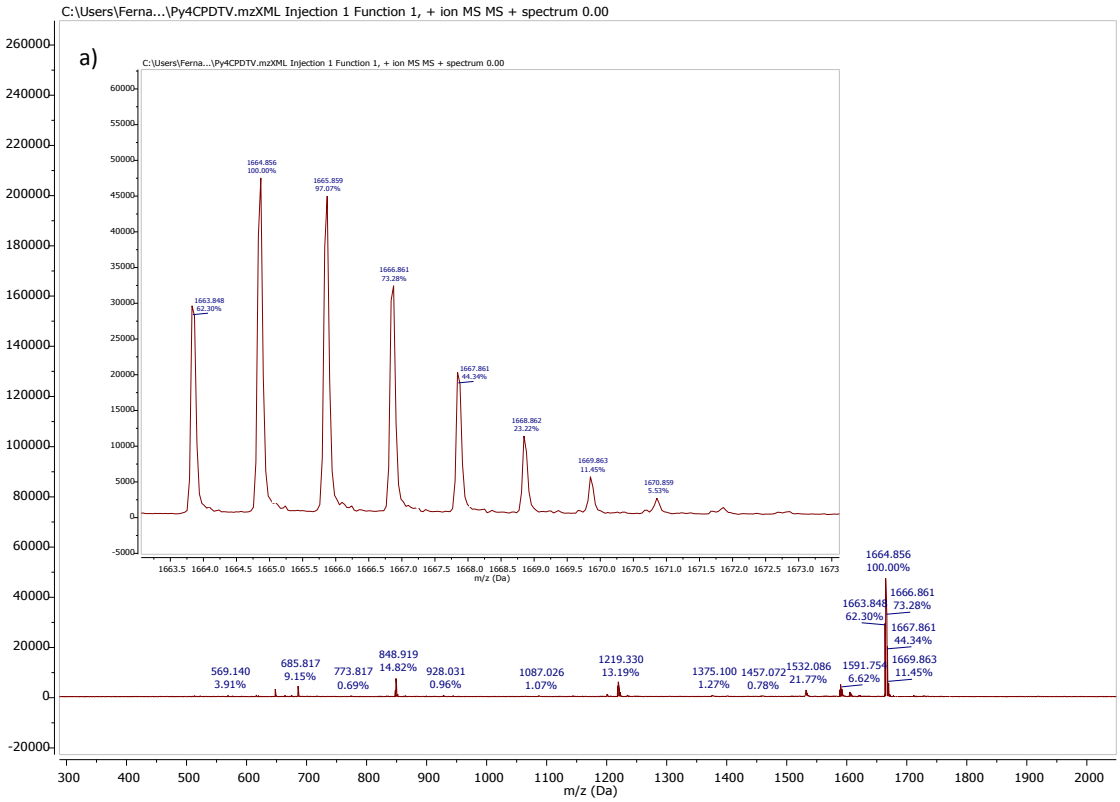

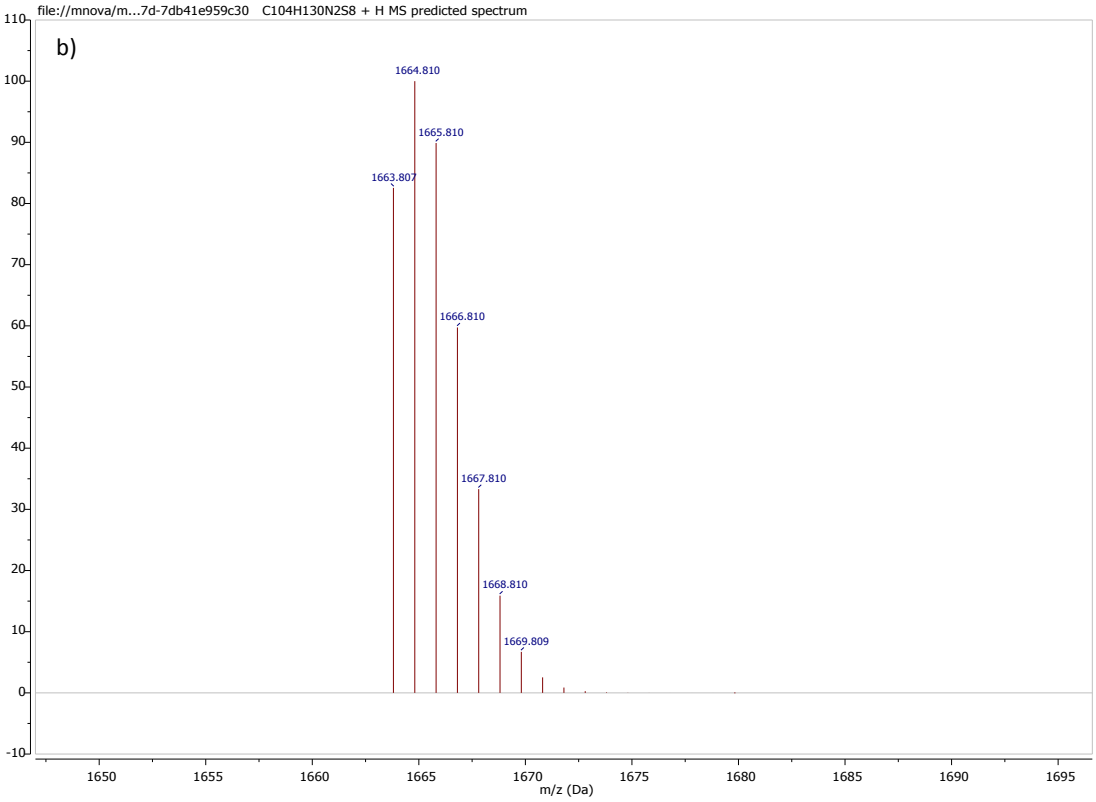


**Figure S27.** a) MS (MALDI-TOF) spectrum and isotopic distribution of compound **Py4CPDTV (3d)** and b) MS (MALDI-TOF) theoretical for compound **Py4CPDTV (3d)** [M+].

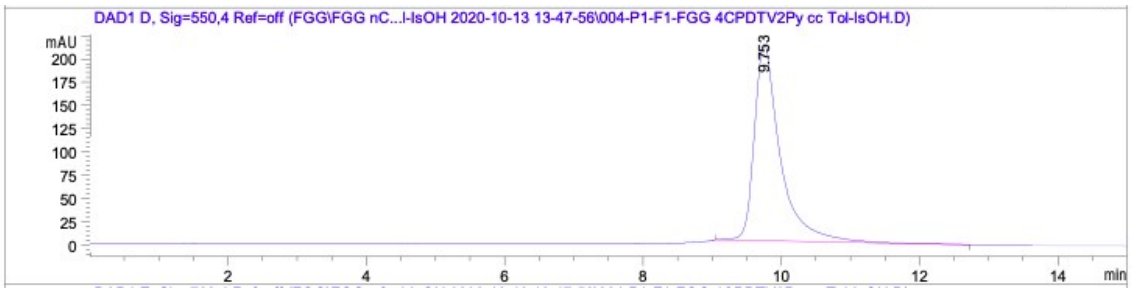


**Figure S28.** HPLC profile of compound **Py4CPDTV (3d)**. Conditions: HPLC column: Buckyprep (4.6ID x 250 mm)), Toluene/Isopropanol (97:3) as eluent (1mL/min); λ=550 nm; 25 °C.

## Part 4. Electrochemistry

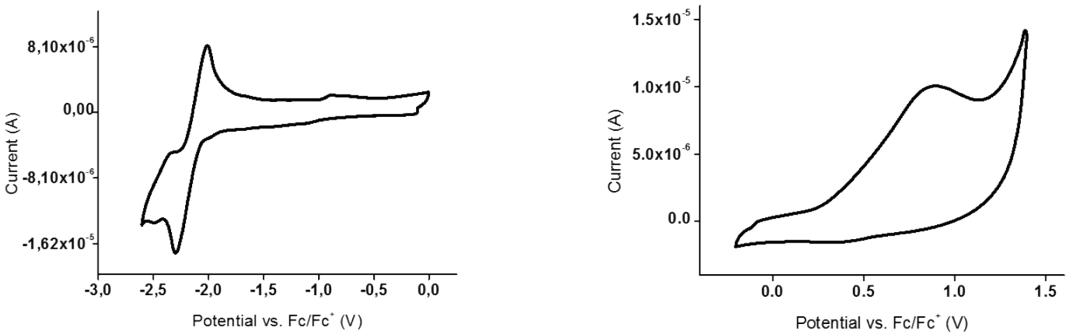


**Figure S29.** Cyclic Voltammetry for oligomer **Py1CPDTV (3a)**.

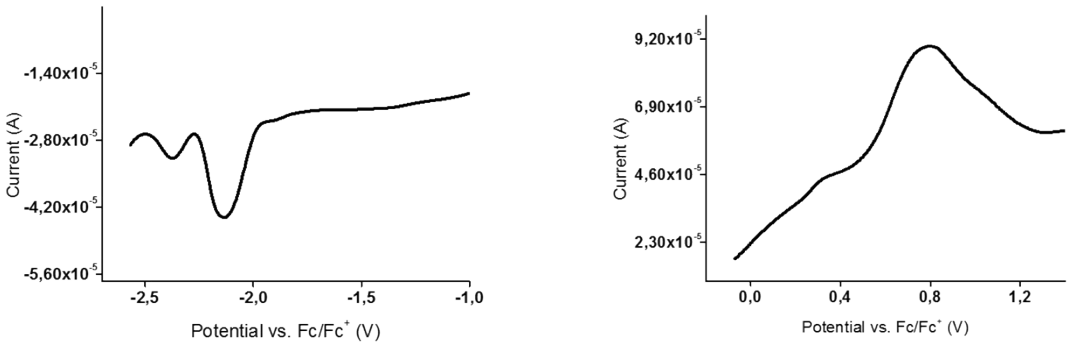


**Figure S30.** Oyster-Young Square Wave Voltammetry for oligomer **Py1CPDTV (3a)**.

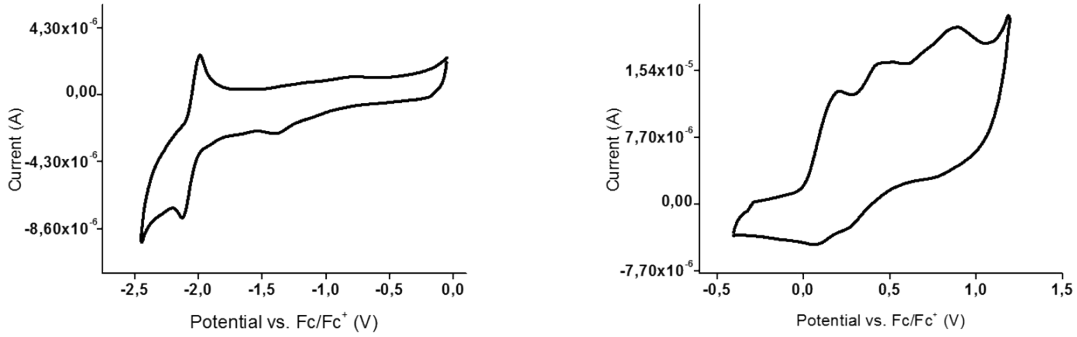


**Figure S31.** Cyclic Voltammetry for oligomer **Py2CPDTV (3b)**.

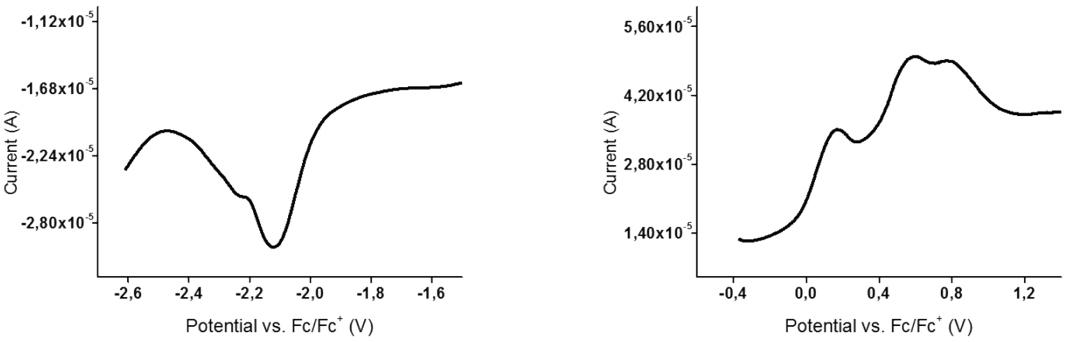


**Figure S32.** Oyster-Young Square Wave Voltammetry for oligomer **Py2CPDTV (3b)**.

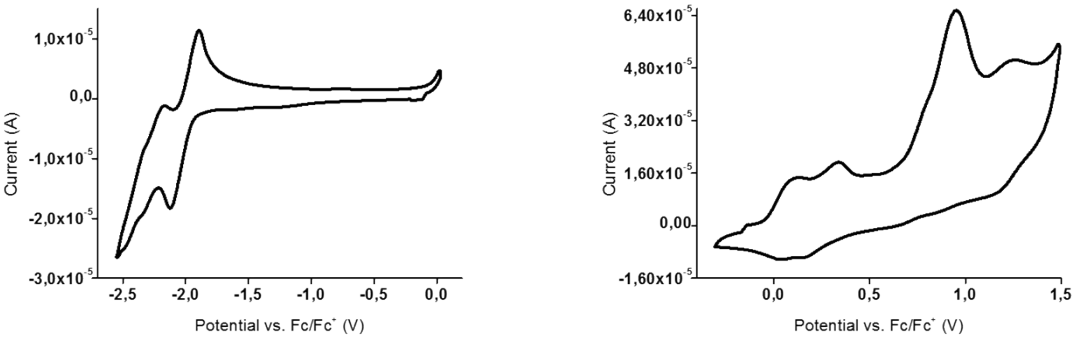


**Figure S33.** Cyclic Voltammetry for oligomer **Py3CPDTV (3c)**.

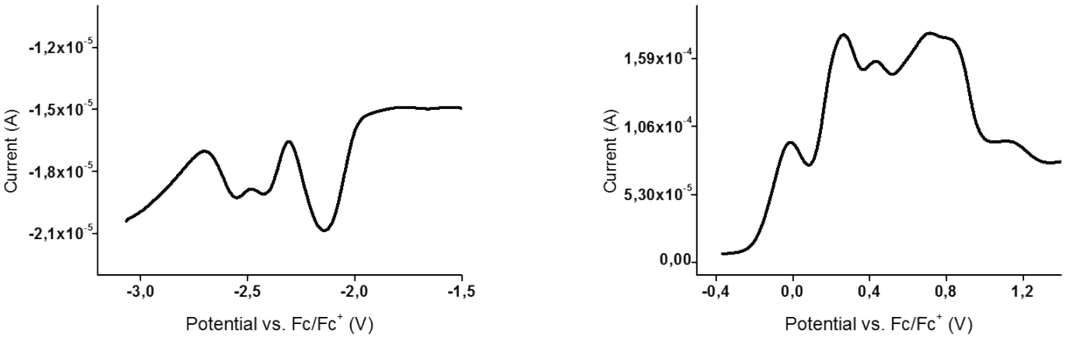


**Figure S34.** Oyster-Young Square Wave Voltammetry for oligomer **Py3CPDTV (3c)**.

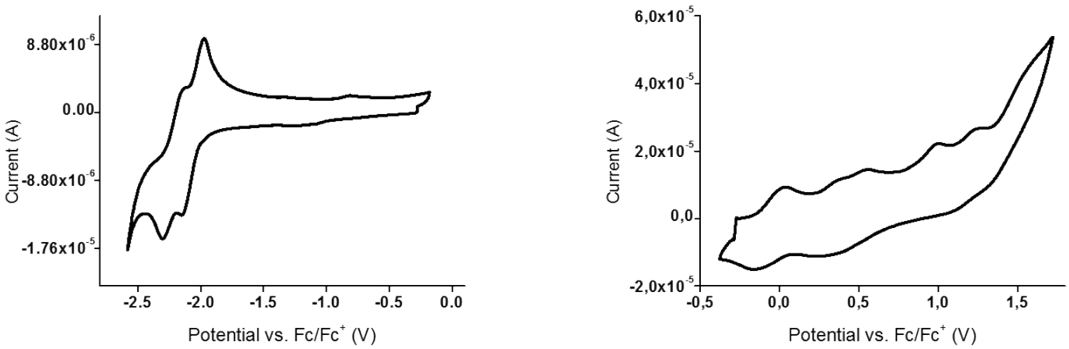


**Figure S35.** Cyclic Voltammetry for oligomer **Py4CPDTV (3d)**.

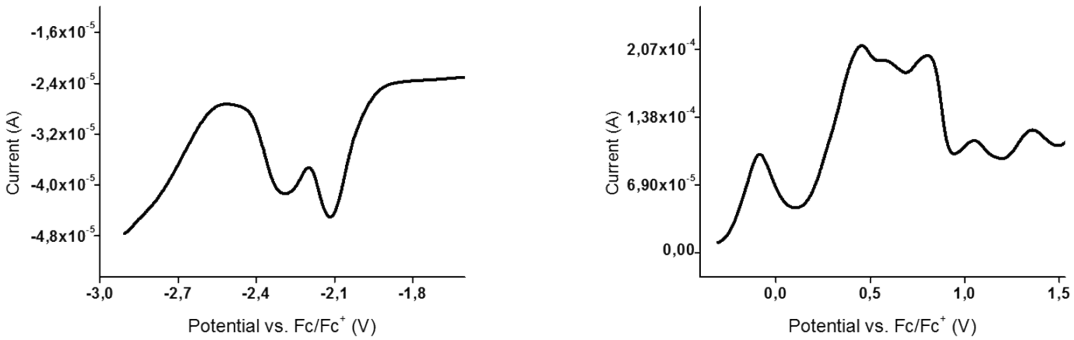


**Figure S36.** Oyster-Young Square Wave Voltammetry for oligomer **Py4CPDTV (3d)**.

**Table S1.** Redox potentials (in V) of **PynCPDTV** oligomers measured from OSWV.

| | $E_{Red}^3$ | $E_{Red}^2$ | $E_{Red}^1$ | $E_{Ox}^1$ | $E_{Ox}^2$ | $E_{Ox}^3$ | $E_{Ox}^4$ | $E_{Ox}^5$ | $E_{Ox}^6$ |
|---|---|---|---|---|---|---|---|---|---|
| **Py1CPDTV** | - | -2.37 | -2.13 | +0.80 | - | - | - | - | - |
| **Py2CPDTV** | - | -2.23 | -2.12 | +0.17 | +0.59 | +0.77 | - | - | - |
| **Py3CPDTV** | -2.55 | -2.43 | -2.14 | -0.01 | +0.26 | +0.43 | +0.71 | +0.82 | - |
| **Py4CPDTV** | - | -2.29 | -2.12 | -0.08 | +0.45 | +0.56 | +0.80 | +1.05 | +1.36 |

Glassy carbon working electrode; Platinum wire counter electrodes; $Ag/AgNO_3$ (0.01 M) reference electrode; scan rate = 100 mV/s. In a 4:1 mixture of *o*-dichlorobenzene (o-DCB) and acetonitrile and 0.1 M of $(n\text{-}Bu)_4NClO_4$ as the supporting electrolyte. The $E_{red}$ and $E_{ox}$ were expressed *vs.* $Fc/Fc^+$ used as external reference.

## Part 5. Theoretical Calculation

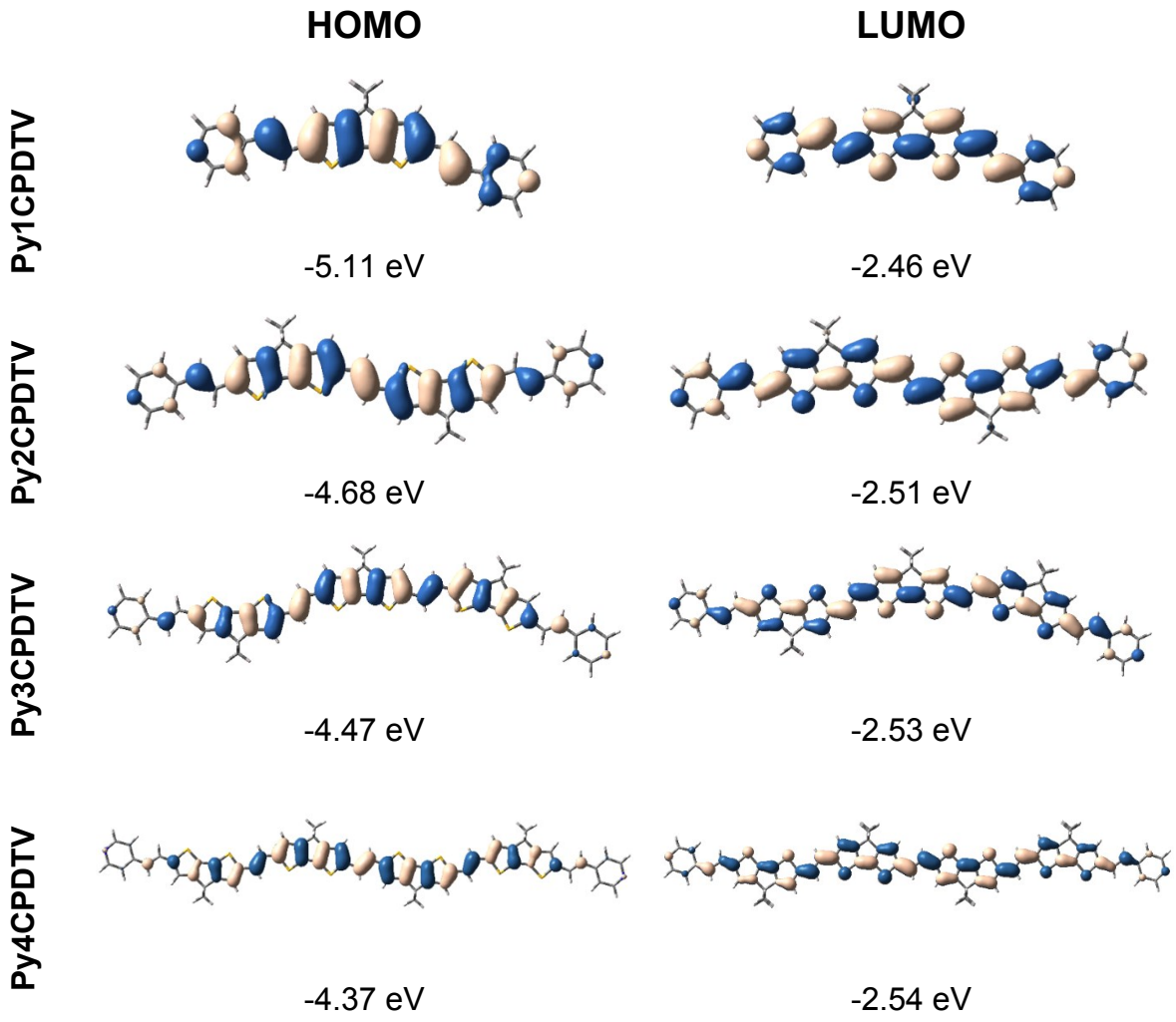


**Figure S37.** DFT calculated Highest Occupied Molecular Orbital (HOMO) and Lowest Unoccupied Molecular Orbital (LUMO) of **PynCPDTV** oligomers. Both orbitals are clearly of π−character.

## Part 6. UV-Vis-NIR Spectrochemistry

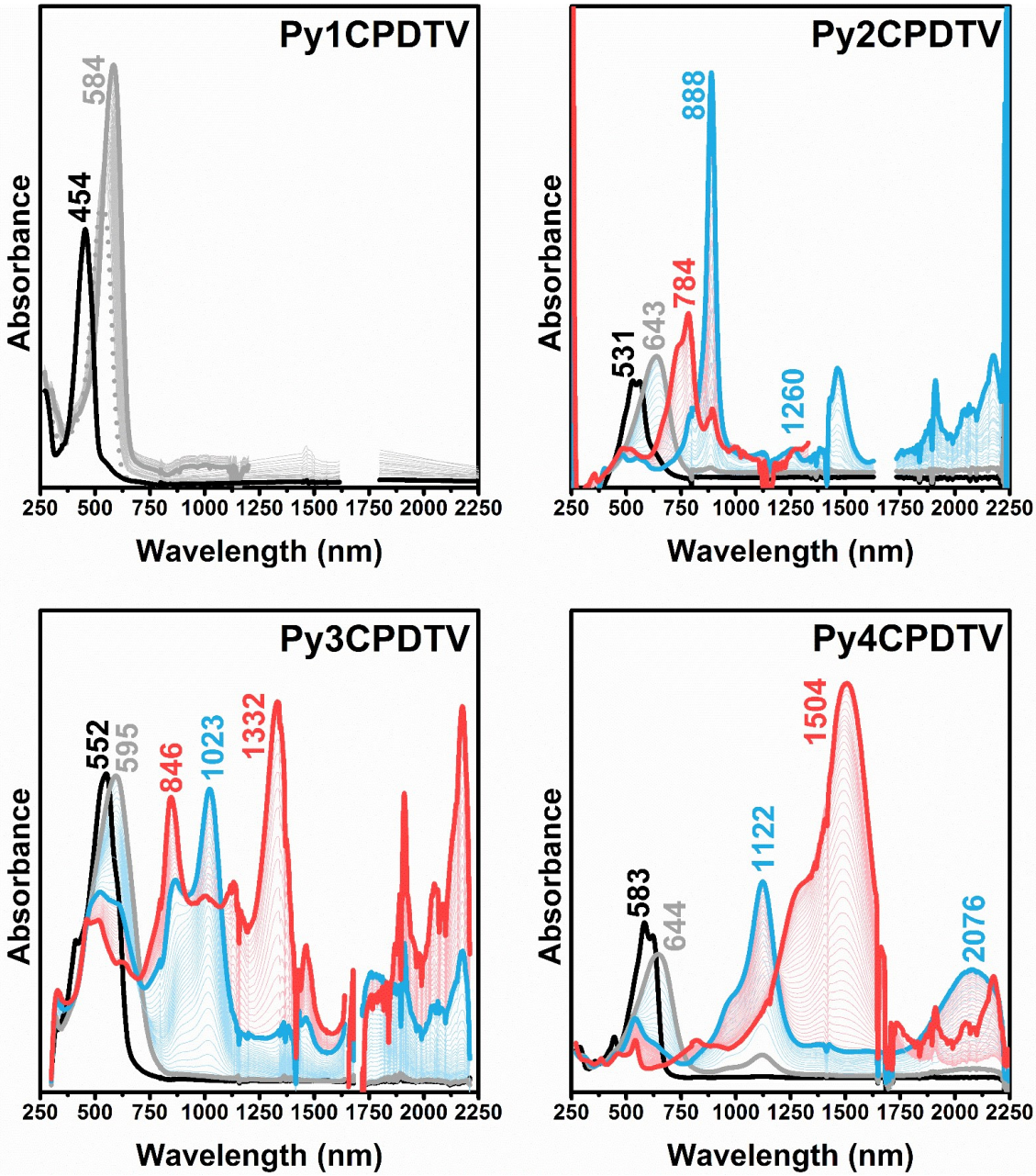


**Figure S38.** UV-Vis-NIR spectrochemical titration with TFA of **PynCPDTV** oligomers $10^{-6}$ M in $CH_2Cl_2$ at room temperature. Black lines: neutral species; grey lines: protonated species; blue lines: radical cations; red lines: dications.

**Table S2.** Absoprtion maxima (nm) of the species obtained upon titration with TFA of **PynCPDTV** oligomers $10^{-6}$ M in DCM at room temperature.

| $\lambda_{max}$ (nm) | Neutral | Mono-protonated | Bis-protonated | Radical Cation | Dication |
|---|---|---|---|---|---|
| **Py1CPDTV** | **454** | **532** | **584** | **—** | **—** |
| **Py2CPDTV** | **531/562** | **—** | **643** | **888**<br>**1260** | **784 (737)** |
| **Py3CPDTV** | **552 (411)** | **—** | **595** | **1023 (867)**<br>**1784** | **846**<br>**1332** |
| **Py4CPDTV** | **583 (621)** | **—** | **644** | **1122 (978)**<br>**2076** | **1504 (1285)** |

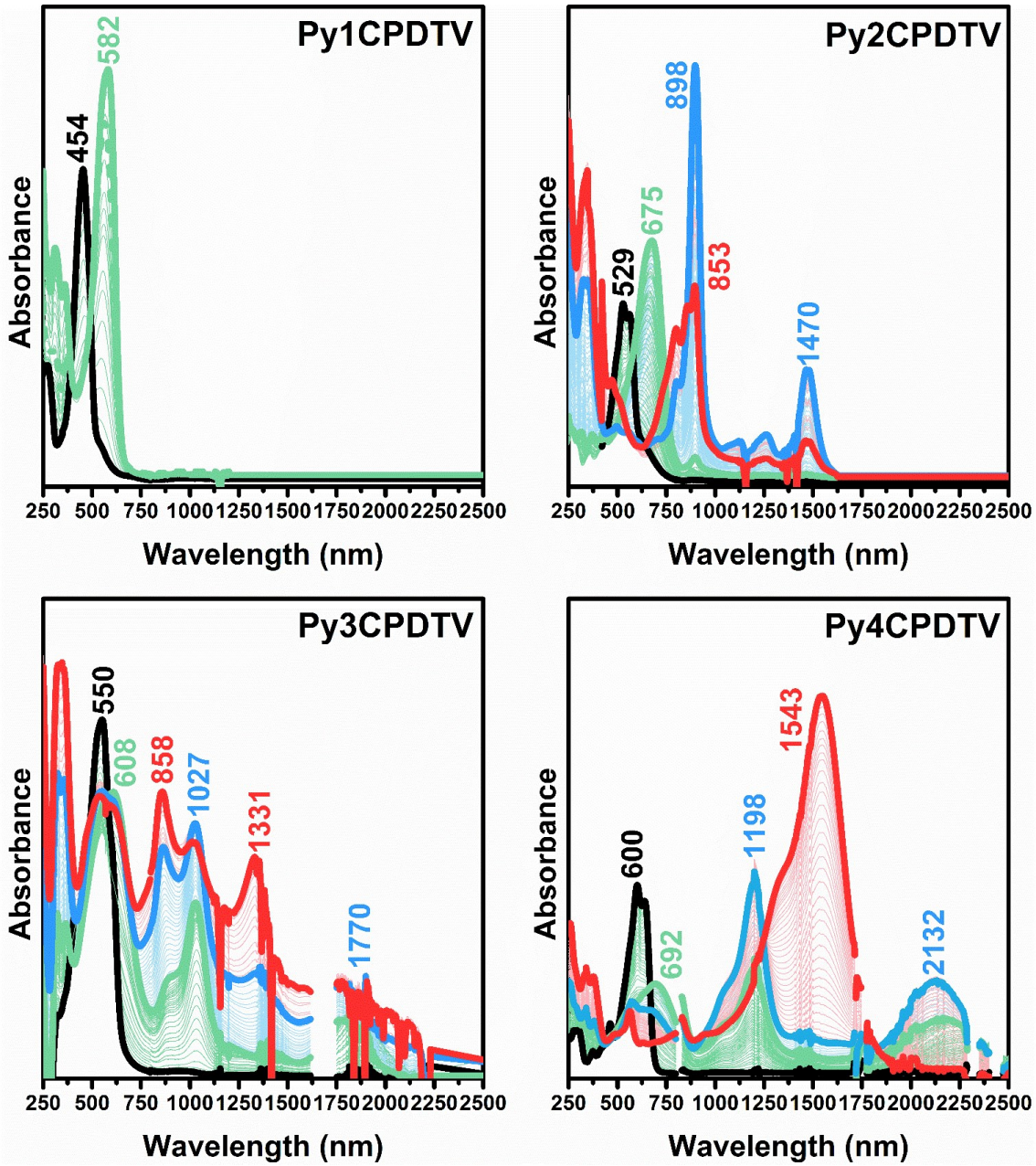


**Figure S39.** UV-Vis-NIR spectrochemical oxidation with $FeCl_3$ of **PynCPDTV** oligomers $10^{-6}$ M in $CH_2Cl_2$ at room temperature. Black lines: neutral species; green lines: coordinated species; blue lines: radical cations; red lines: dications.

**Table S3.** Absoprtion maxima (nm) of the species obtained upon oxidation with $FeCl_3$ of **PynCPDTV** oligomers $10^{-6}$ M in DCM at room temperature.

| $\lambda_{max}$ (nm) | Neutral | Mono-coordinated | Bis-coordinated | Radical Cation | Dication |
|---|---|---|---|---|---|
| **Py1CPDTV** | **454** | **564** | **582** | **—** | **—** |
| **Py2CPDTV** | **529/561** | **—** | **675** | **898 (801)**<br>**1470** | **853 (798)** |
| **Py3CPDTV** | **550 (530)** | **—** | **608** | **1027 (863)**<br>**1770** | **858**<br>**1331** |
| **Py4CPDTV** | **600/637** | **—** | **692** | **1198 (1045)**<br>**2132** | **1543 (1331)** |

## Part 7. Vapochromism Experiments

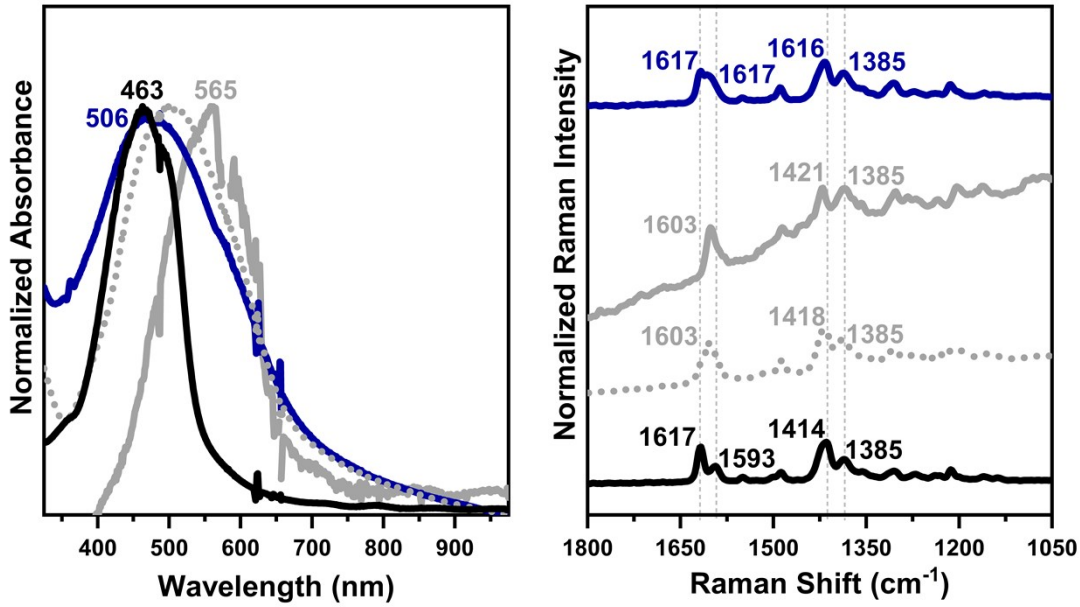


**Figure S40.** Left) Electronic absorption spectra of spin-coated thin films of **Py1CPDTV (3a)** (black line), upon treatment with TFA acid (dashed and solid grey lines, at different exposition times) and the recovered spectrum upon treatment with $NH_3$ vapor (dark blue line). Right) The corresponding 1064 nm FT-Raman spectra.

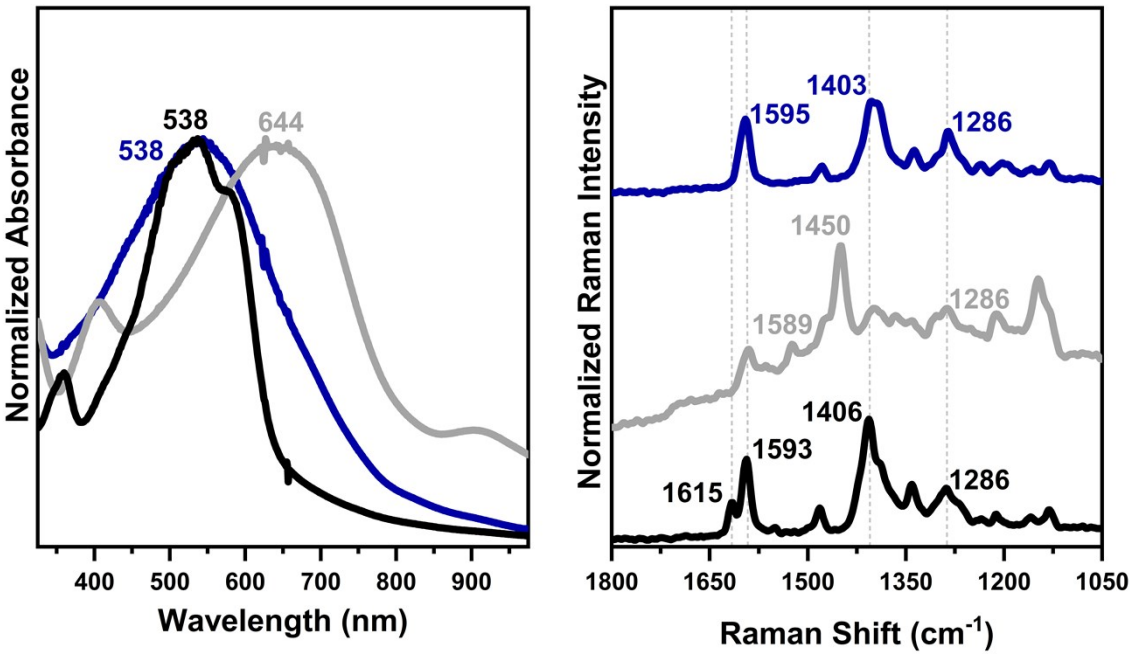


**Figure S41.** Left) Electronic absorption spectra of spin-coated thin films of **Py2CPDTV (3b)** (black line), upon treatment with TFA acid (grey line) and the recovered spectrum upon treatment with $NH_3$ vapor (dark blue line). Right) The corresponding 1064 nm FT-Raman spectra.

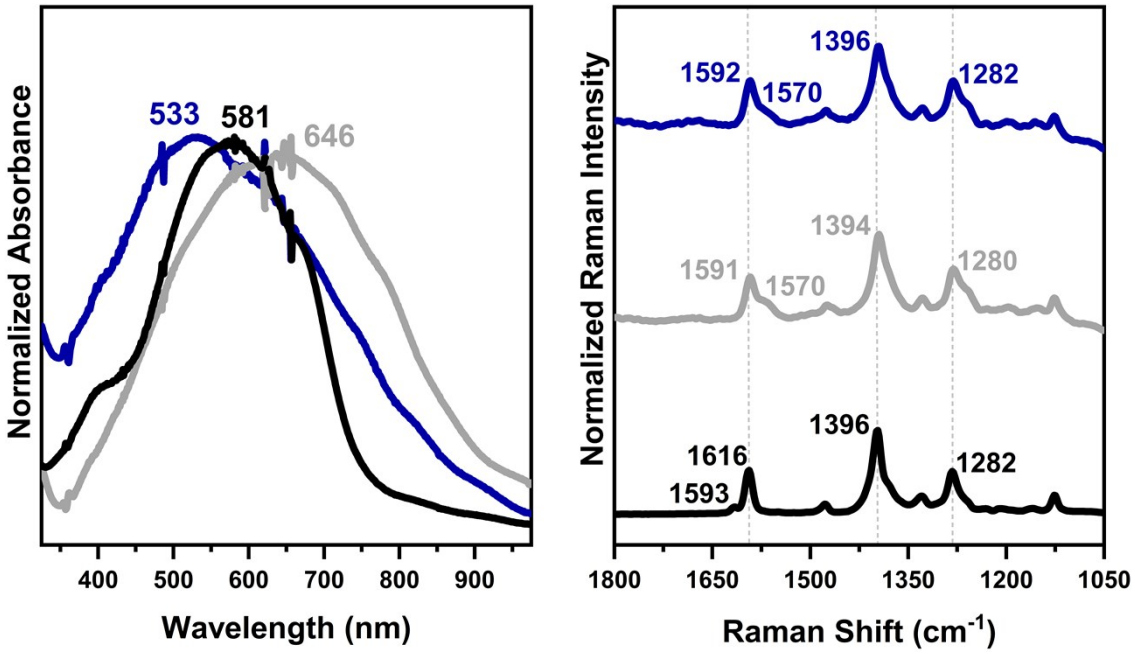


**Figure S42.** Left) Electronic absorption spectra of spin-coated thin films of **Py4CPDTV (3d)** (black line), upon treatment with TFA acid (grey line) and the recovered spectrum upon treatment with $NH_3$ vapor (dark blue line). Right) The corresponding 1064 nm FT-Raman spectra.

## Part 8. Electrical properties: Organic Field Effect Transistors

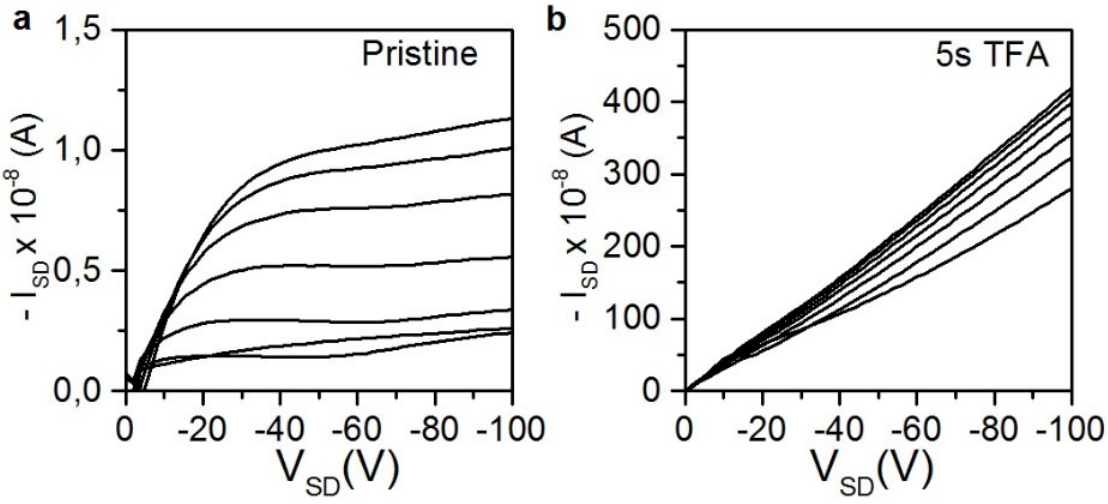


**Figure S43.** Output ($I_{SD}$-$V_{SD}$) plot data for **Py4CPDTV (3d)**-based devices. (a) Pristine film and (b) After exposition to TFA for 5-10 s.

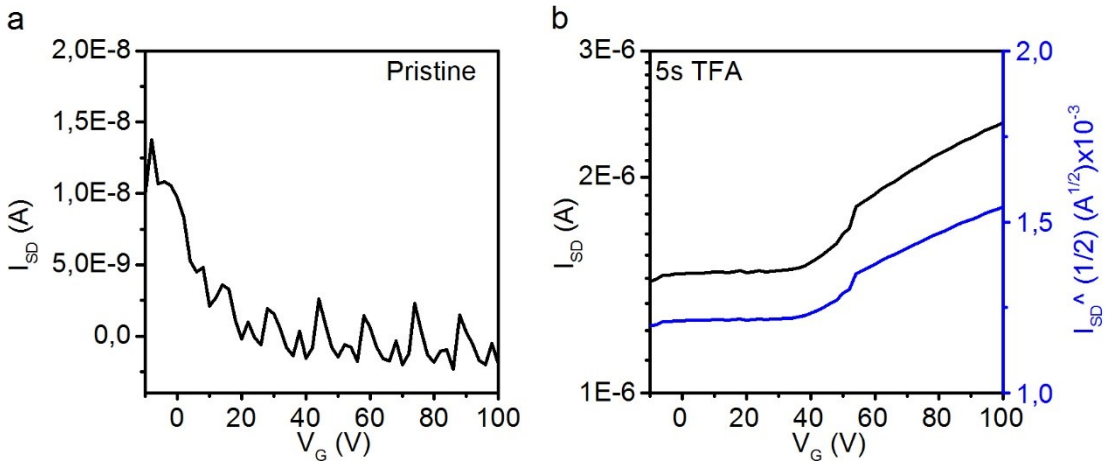


**Figure S44.** $I_{SD}$-$V_G$ plot data for **Py4CPDTV (3d)**-based devices measured at positive bias. (a) Pristine film and (b) After exposition to TFA for 5-10 s.

## References

1. Gaussian 16, Revision B.01, M. J. Frisch, G. W. Trucks, H. B. Schlegel, G. E. Scuseria, M. A. Robb, J. R. Cheeseman, G. Scalmani, V. Barone, G. A. Petersson, H. Nakatsuji, X. Li, M. Caricato, A. V. Marenich, J. Bloino, B. G. Janesko, R. Gomperts, B. Mennucci, H. P. Hratchian, J. V. Ortiz, A. F. Izmaylov, J. L. Sonnenberg, D. Williams-Young, F. Ding, F. Lipparini, F. Egidi, J. Goings, B. Peng, A. Petrone, T. Henderson, D. Ranasinghe, V. G. Zakrzewski, J. Gao, N. Rega, G. Zheng, W. Liang, M. Hada, M. Ehara, K. Toyota, R. Fukuda, J. Hasegawa, M. Ishida, T. Nakajima, Y. Honda, O. Kitao, H. Nakai, T. Vreven, K. Throssell, J. A., Jr. Montgomery, J. E. Peralta, F. Ogliaro, M. J. Bearpark, J. J. Heyd, E. N. Brothers, K. N. Kudin, V. N. Staroverov, T. A. Keith, R. Kobayashi, J. Normand, K. Raghavachari, A. P. Rendell, J. C. BurantS. S. Iyengar, J. Tomasi, M. Cossi, J. M. Millam, M. Klene, C. Adamo, R. Cammi, J. W. Ochterski, R. L. Martin, K. Morokuma, O. Farkas, J. B. Foresman, D. J. Fox, Gaussian, Inc., Wallingford CT, 2016.

2. A. D. Becke, *J. Chem. Phys*., 1993, **98**, 1372.

3. M. M. Francl, W. J. Pietro, W. J. Hehre, J. S. Binkley, M. S. Gordon, D. J. Defrees, J. A. Pople, *J. Chem. Phys.,* 1982, **77**, 3654.

4. T. Gadzikwa, G. Lu, C. L. Stern, S. R. Wilson, J. T. Hupp, S. T. Nguyen, *Chem*. *Commun*., 2008, 5493.

5. B. R. Baker, M. H. Doll, *J*. *Med*. *Chem*., 1971, **14**, 793.

6. P. M. Burrezo, R. Domínguez, J. L. Zafra, T. M. Pappenfus, P. de la Cruz, L. Welte, D. E. Janzen, J. T. López Navarrete, F. Langa, J. Casado, *Chem*. *Sci*., 2017, **8**, 8106.